Study of spin transport and novel quantum states in multilayers from organic and oxide materials

C. Bernhard

Department of Physics and Fribourg Center for Nanomaterials (FriMat), University of Fribourg, CH-1700 Fribourg, Switzerland

christian.bernhard@unifr.ch

UNIVERSITAS FRIBURGENSIS

MaNEP SWITZERLAND

frimat

FK group

Research Topics

- Oxides with strongly correlated electrons (high T_c, CMR, etc.)
- Oxide multilayers with competing orders
- Spin-injection in organic spin-valves

Experimental Techniques

- Thin film growth with pulsed laser deposition (PLD) and thermal evaporation.
- Spectroscopic Ellipsometry (FIR-UV)
- Neutron Reflectometry
- Muon-Spin-Rotation

Measuring current induced spin polarisation in organic spin-valves

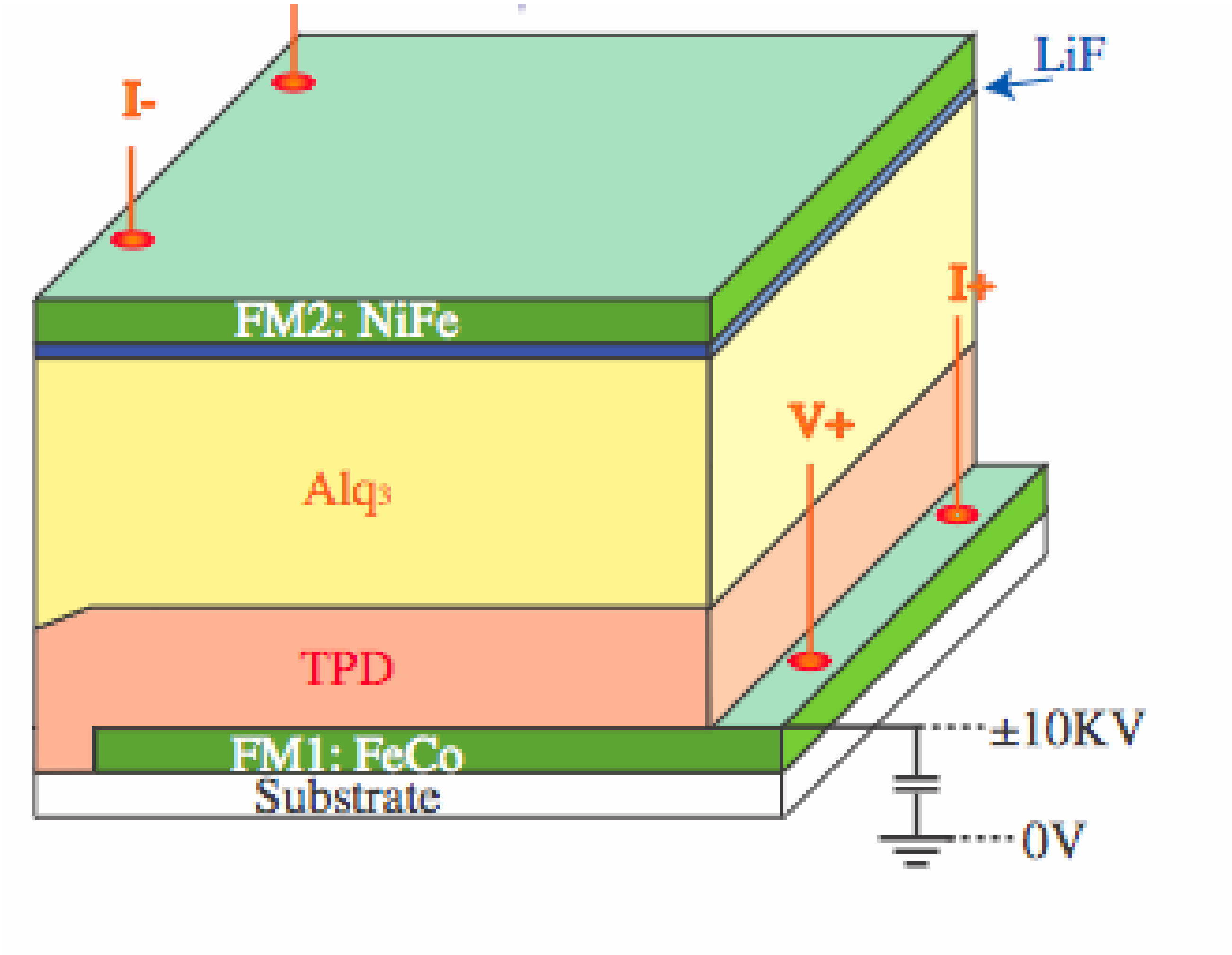

Alan Drew

Leo Schulz

Sample grown at Queen Mary College, London, UK

Giant Magneto Resistance (GMR) in metallic FM/N/FM multilayers – spin dependent confinement

Magnetic exchange-splitting

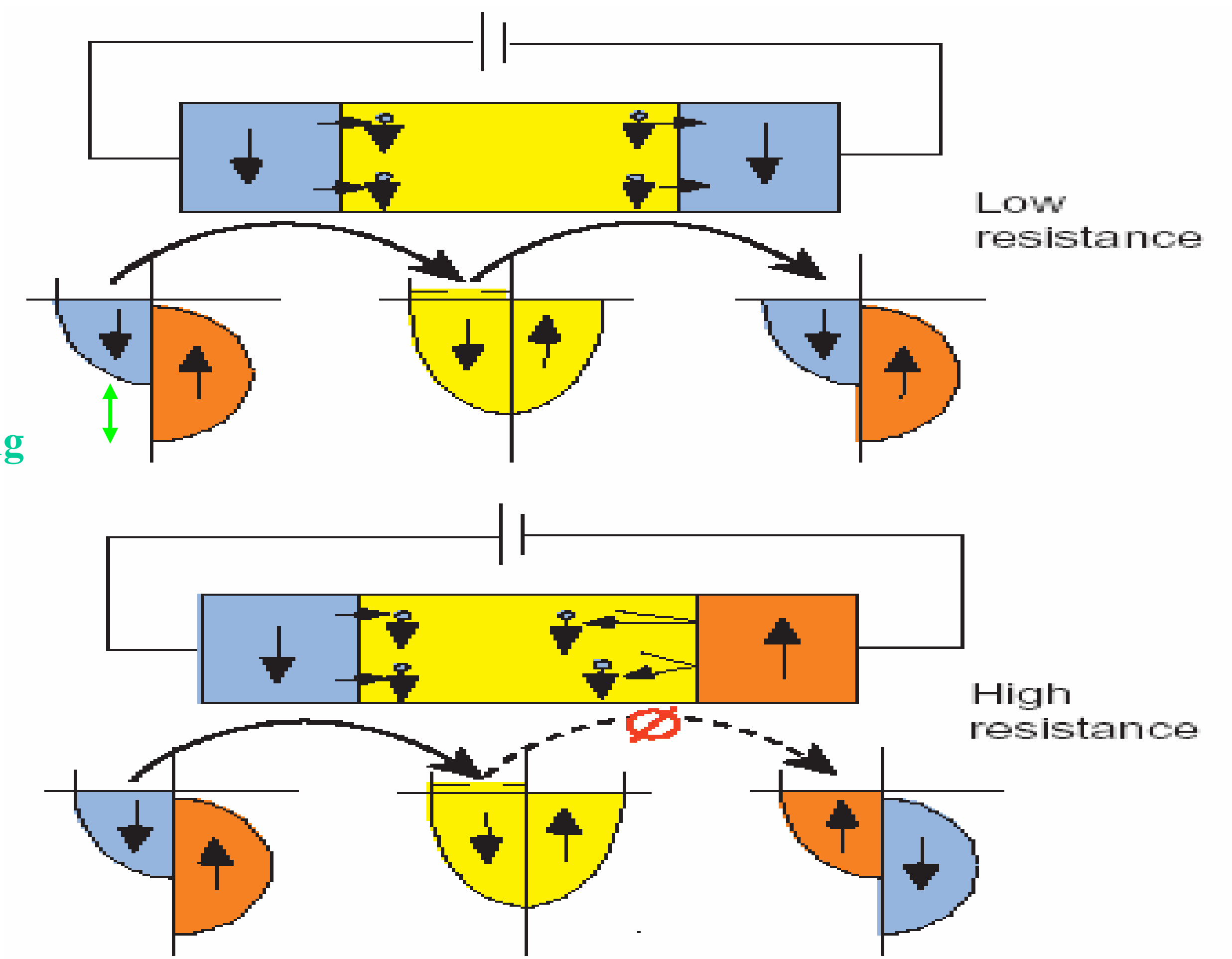

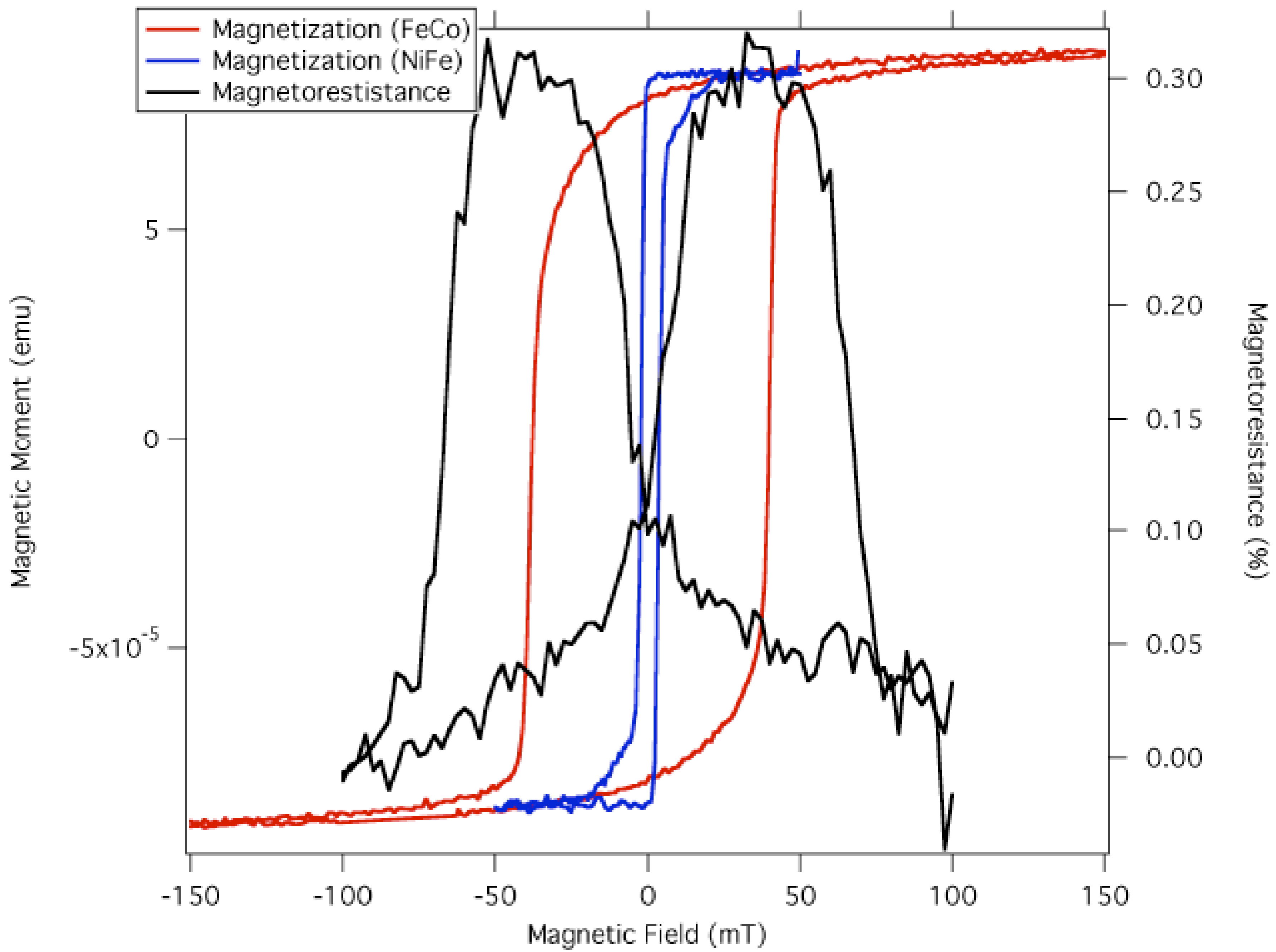

Magnetization (FeCo)
Magnetization (NiFe)
Magnetorestistance
Magnetic Moment (emu)
5
0
-5x10-5
0.30
0.25
0.20
0.15
0.10
0.05
0.00
Magnetoresistance (%)
-150
-100
-50
0
50
100
150
Magnetic Field (mT)

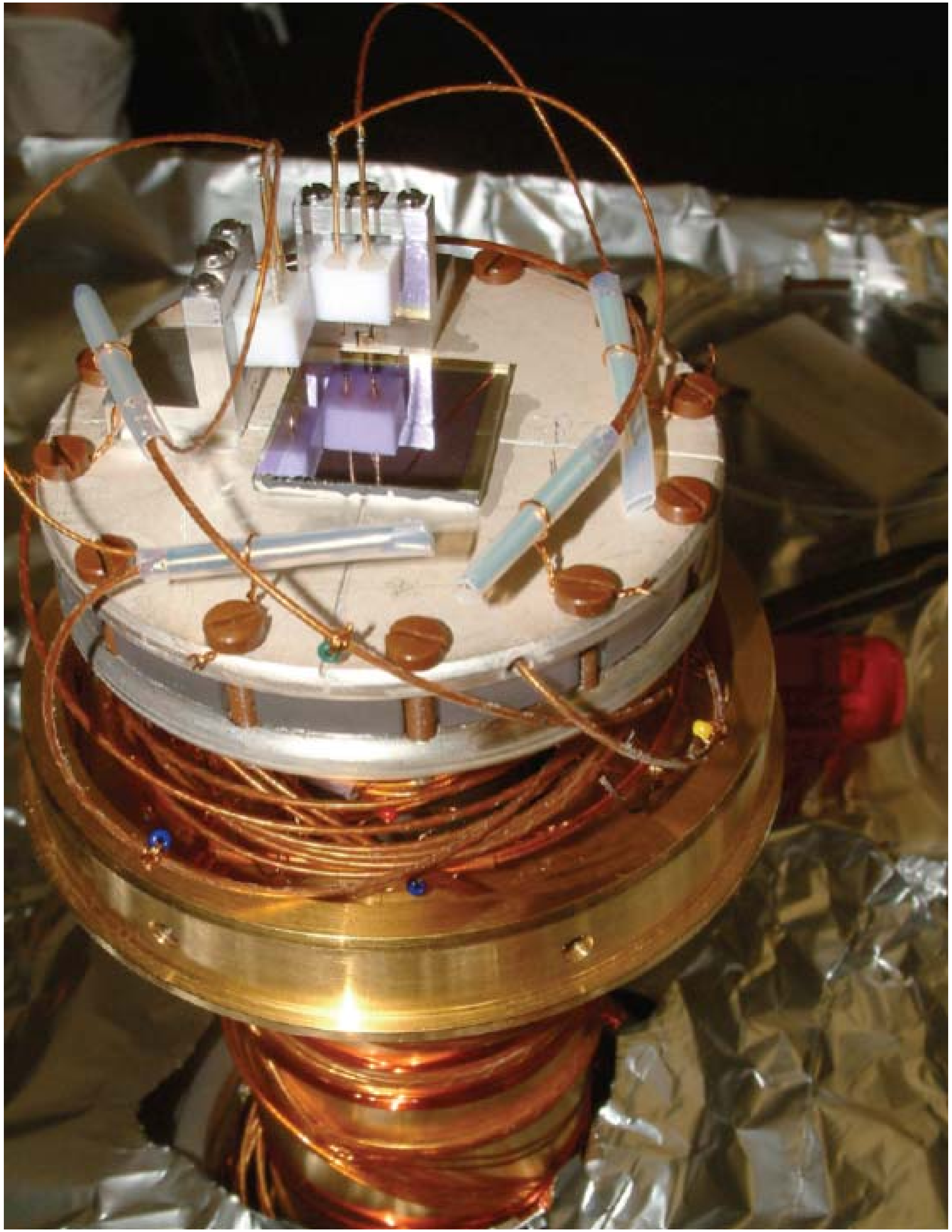

Myon-Spin-Rotation (μSR) @ PSI

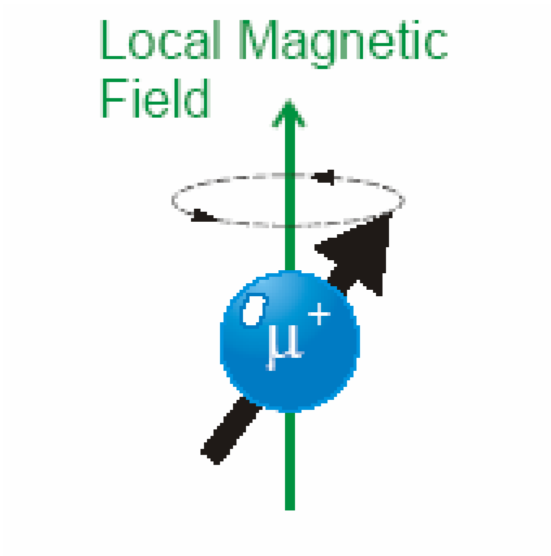

Perferential direction for positron emission

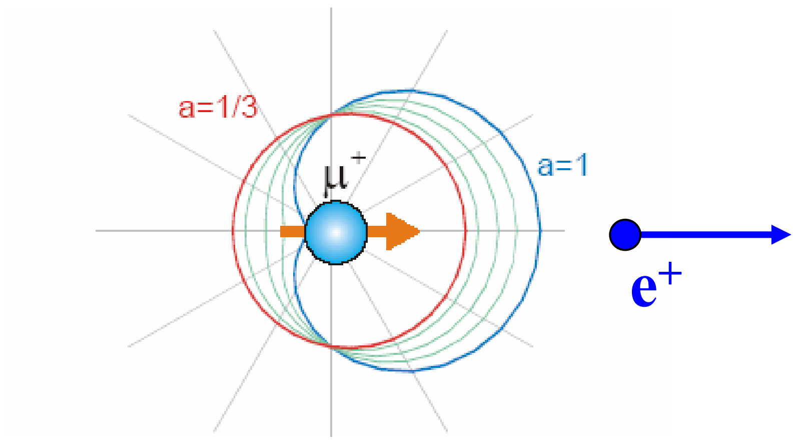

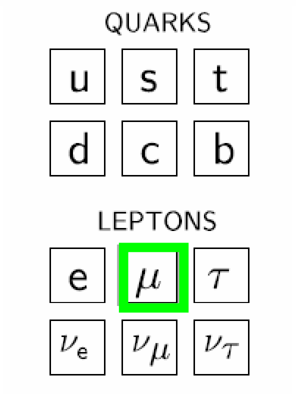

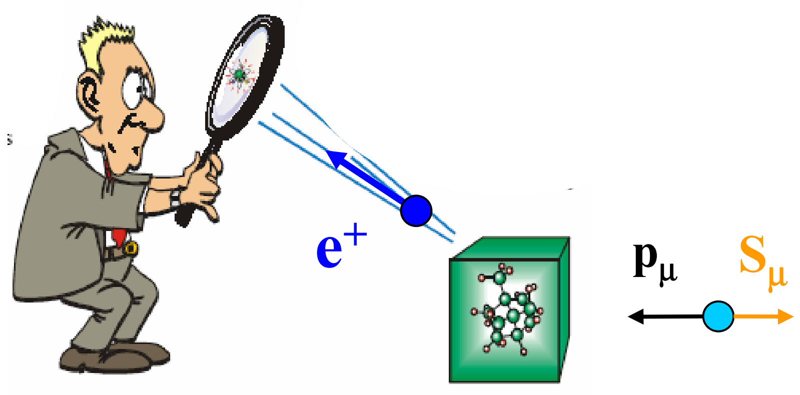

Typical μSR setup

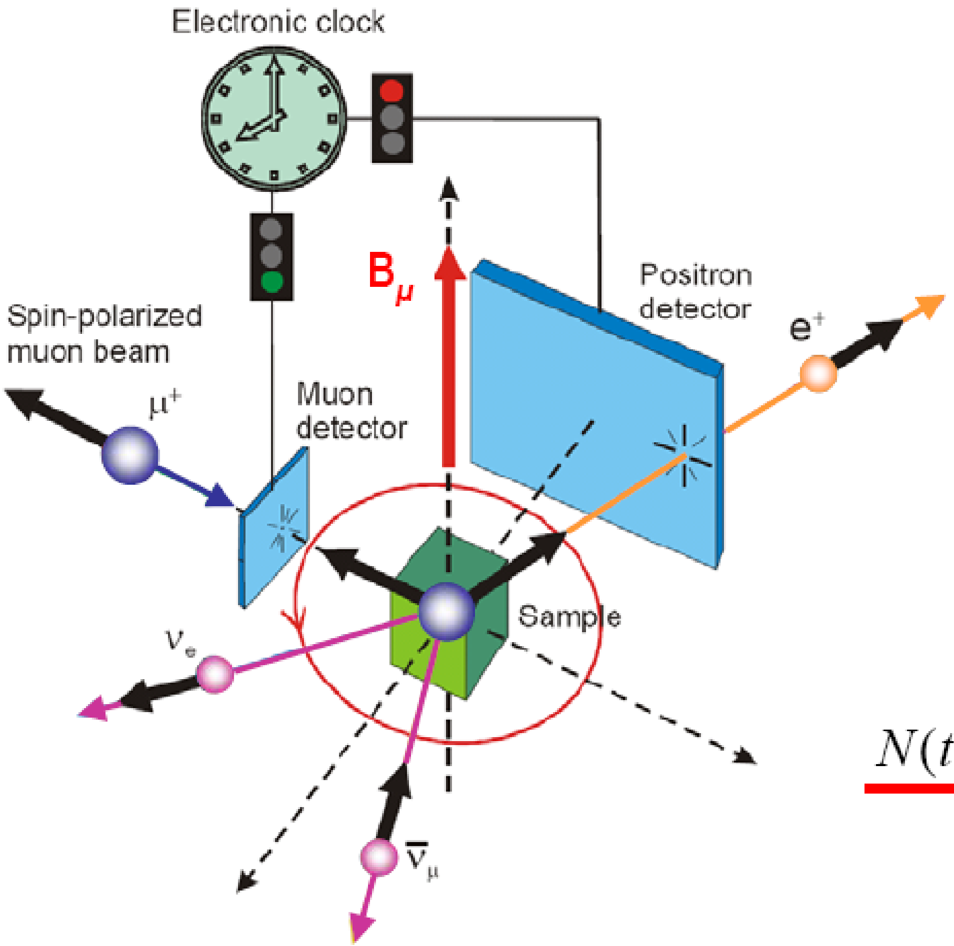

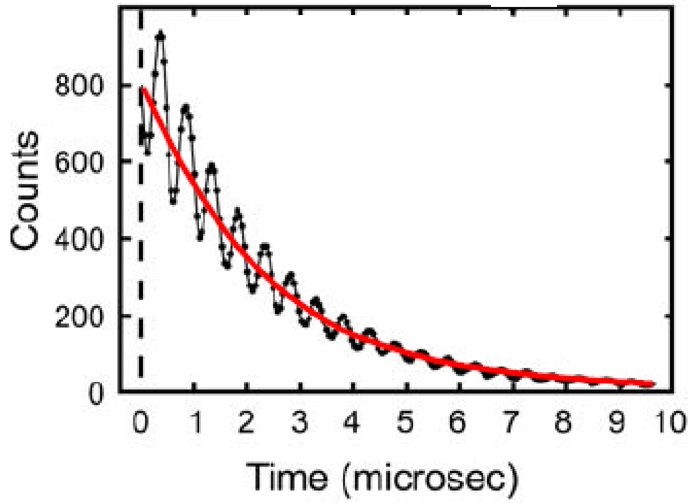

$$N(t) = B + N_0 \exp(-t / \tau_\mu)$$

$\mathbf{B}_\mu$ internal or external field

μSR spectra

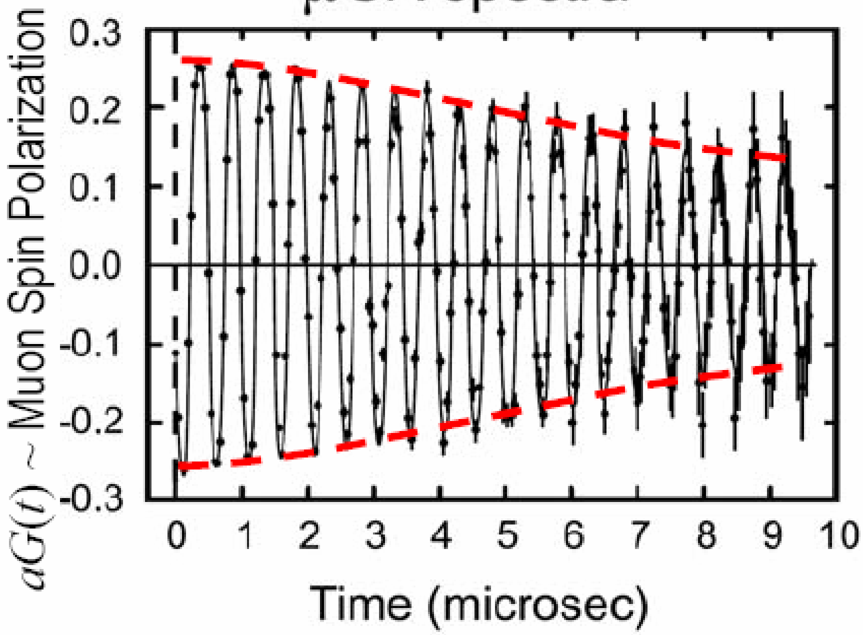

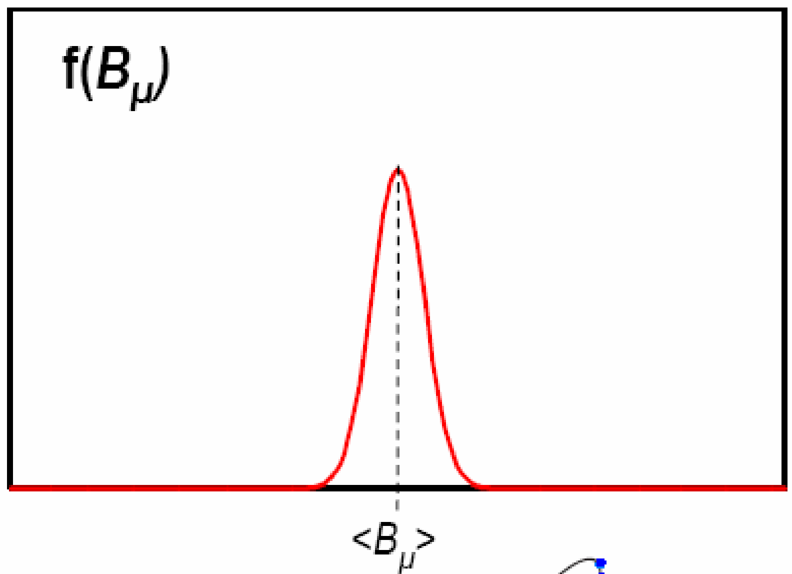

$$G(t) = \int f(\mathbf{B}_\mu)\left[\cos^2\theta + \sin^2\theta\cos(\gamma_\mu B_\mu t)\right] d\mathbf{B}_\mu$$

θ angle between magnetic field and muon polarization at $t = 0$
By choosing θ = 90°, one obtains:

$$G(t) = \int f(\mathbf{B}_\mu)\cos(\gamma_\mu B_\mu t) d\mathbf{B}_\mu$$

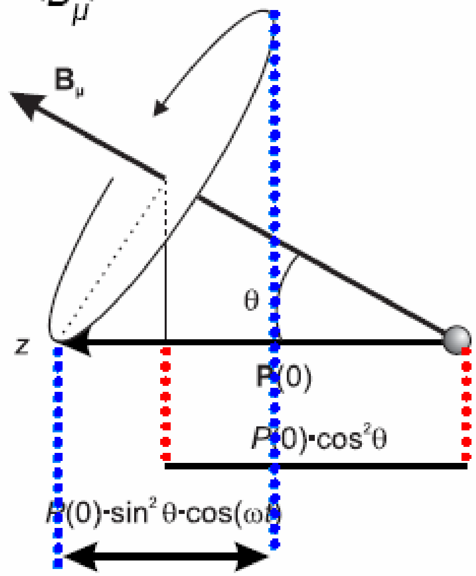

Low energy μ^+ beam and set-up for LE-μSR

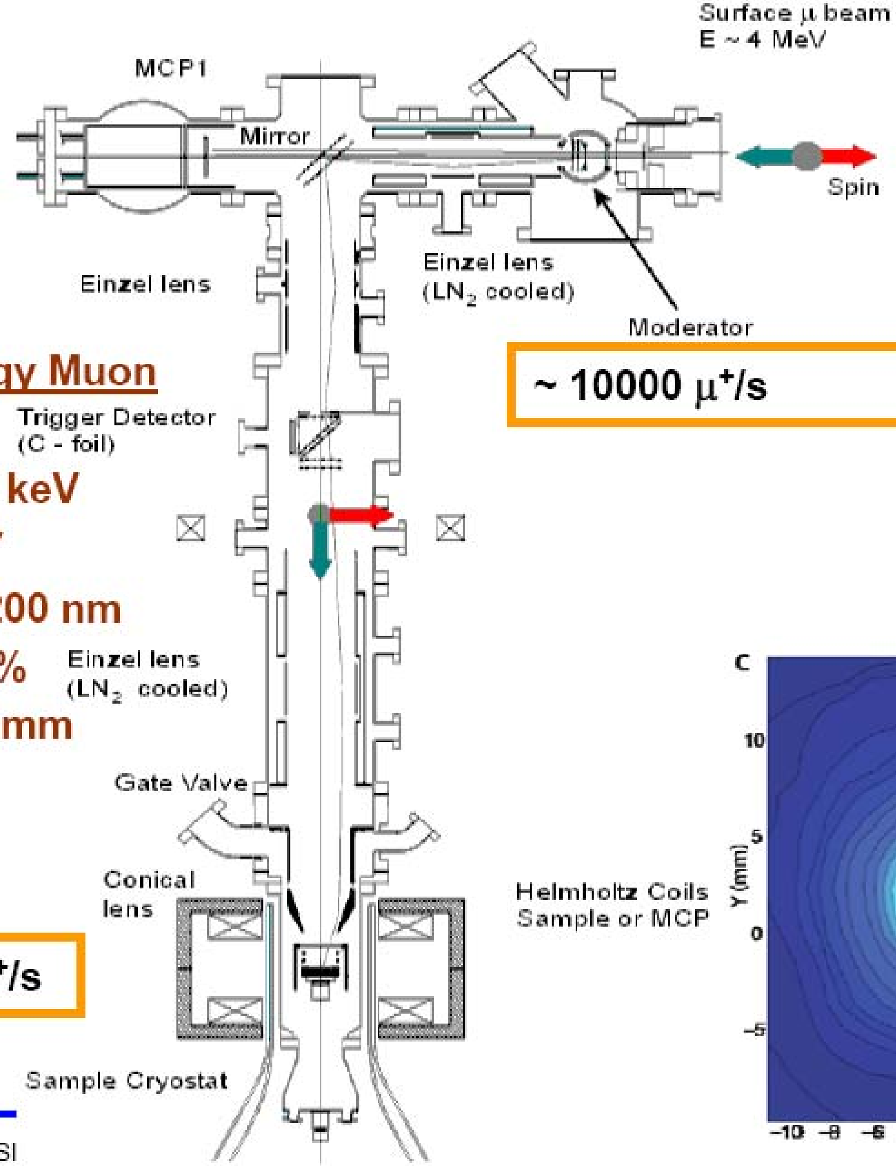

~$1.7 \cdot 10^8$ μ^+/s

from new μE4 beam line

- UHV system (~10^{-10} mbar)
- Electrostatic transport, focussing and energy selection.
- All transport elements LN_2 cooled

~ 10000 μ^+/s

Polarized Low Energy Muon Beam

Energy:	0.5-30 keV
ΔE:	400 eV
Depth:	~ 1 – 200 nm
Polarization	~ 100 %
Beam Spot:	10-20 mm

~ 4200 μ^+/s

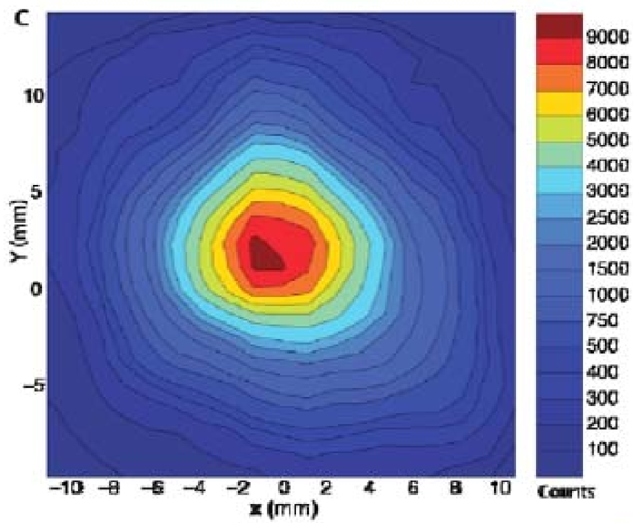

Niederenergetische Muonen @ Paul-Scherrer-Institut

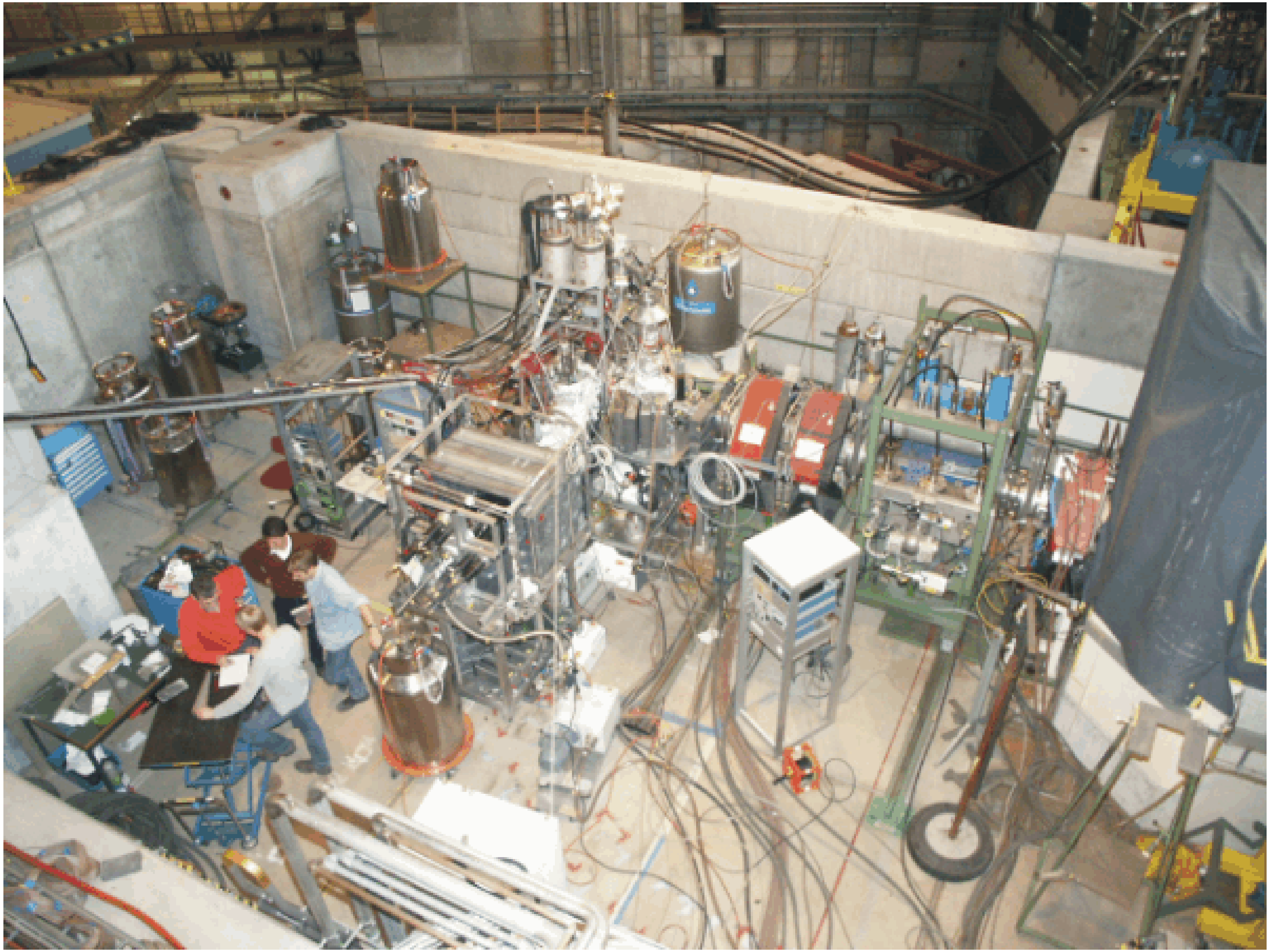

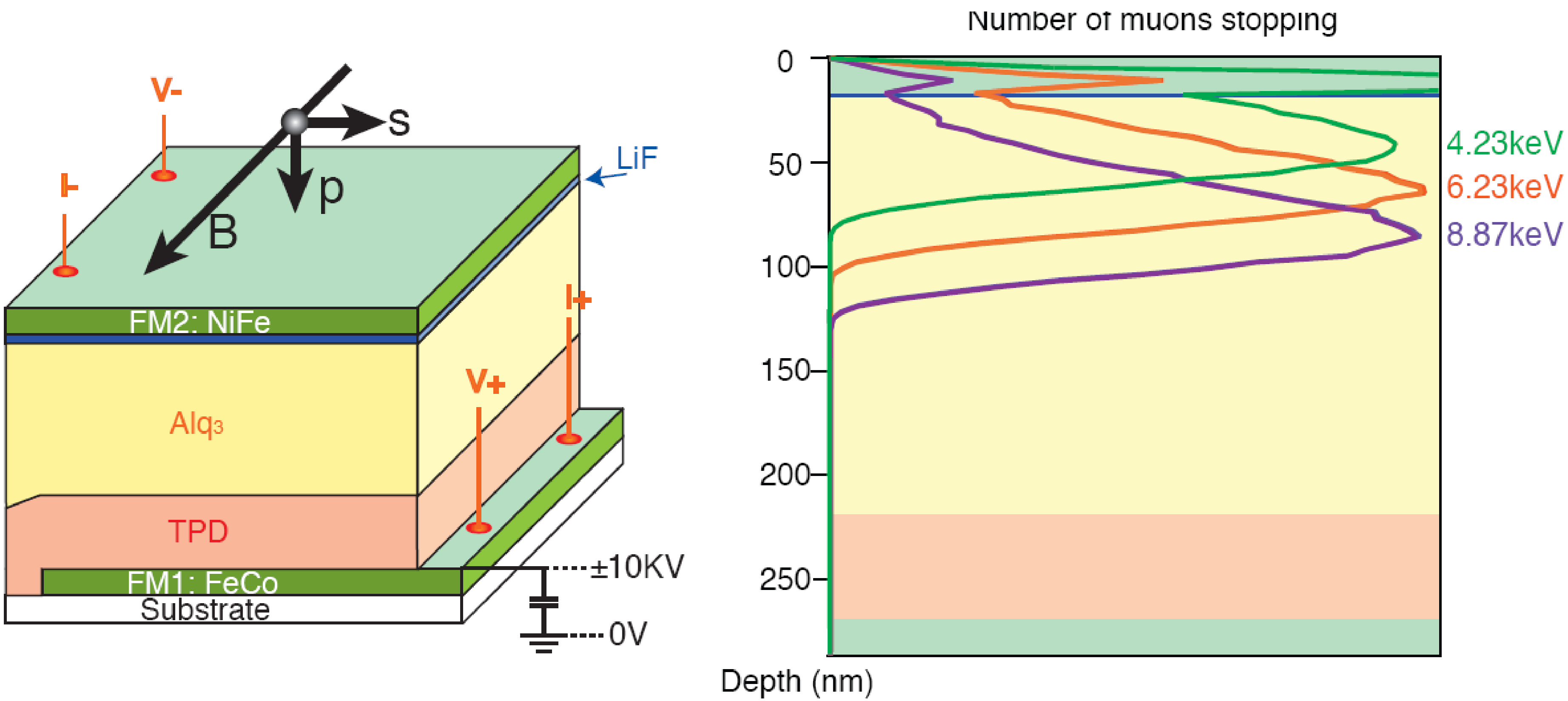
V-
I-
s
p
B
LiF
FM2: NiFe
Alq3
I+
V+
TPD
FM1: FeCo
Substrate
±10KV
0V
Number of muons stopping
0
50
100
150
200
250
4.23keV
6.23keV
8.87keV
Depth (nm)

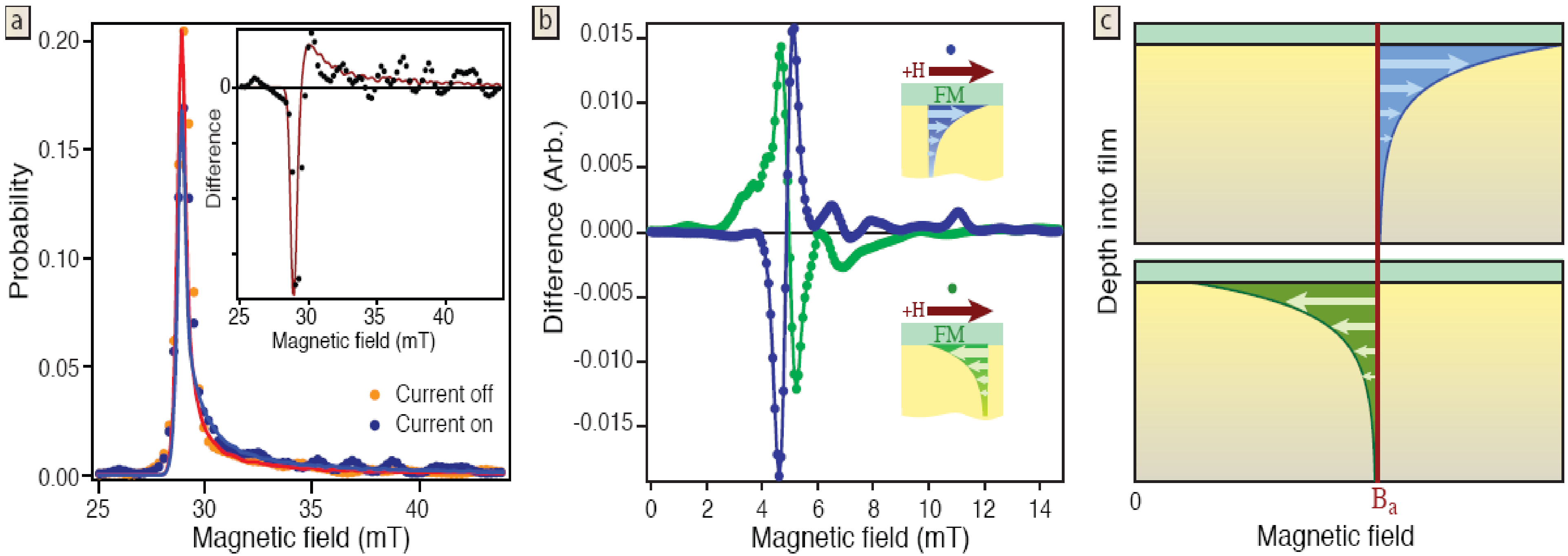
a
Probability
Magnetic field (mT)
Current off
Current on
Difference
Magnetic field (mT)
b
Difference (Arb.)
Magnetic field (mT)
+H
FM
+H
FM
c
Depth into film
Magnetic field
0
Ba

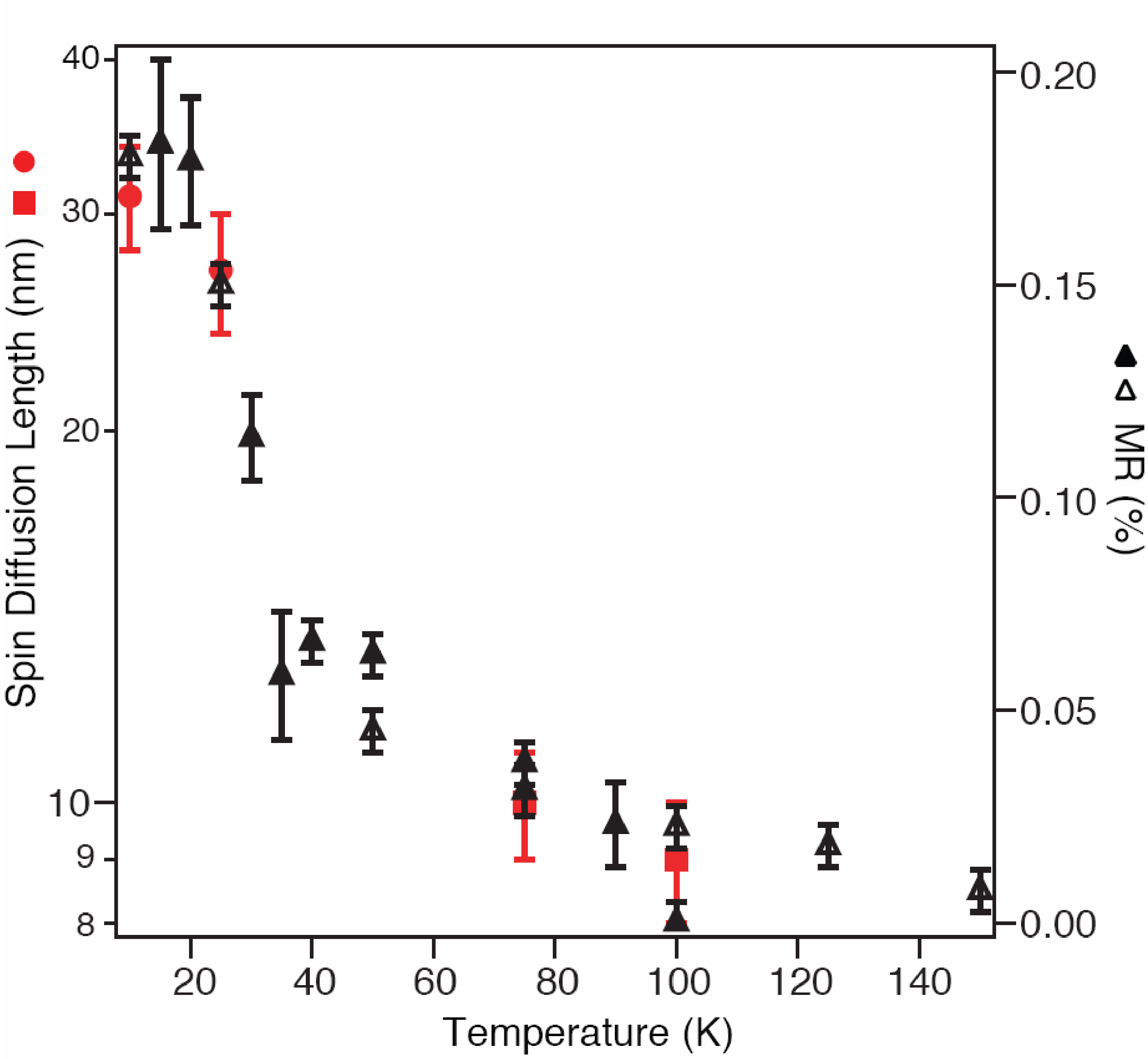

Spin Diffusion Length (nm)
40
30
20
10
9
8
20
40
60
80
100
120
140
Temperature (K)
0.20
0.15
0.10
0.05
0.00
MR (%)

Conclusion

We can measure quantitatively and depth-resolved the current-induced spin polarisation in the active (buried) layers of a functional organic spin-valve.

We can distinguish between interface effects and spin transport effects in the individual layers.

What else can we do?

PLD growth of oxide multilayers with competing orders

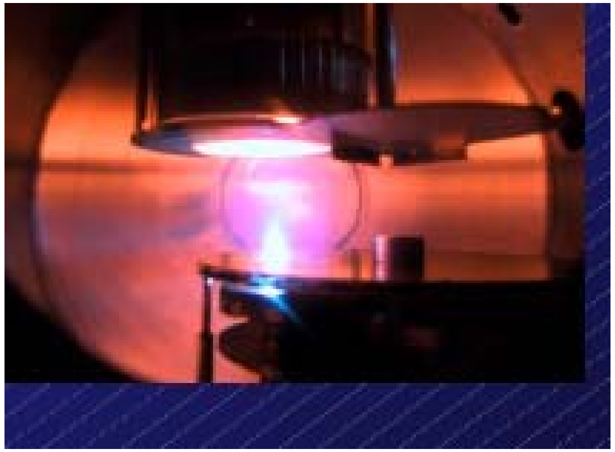

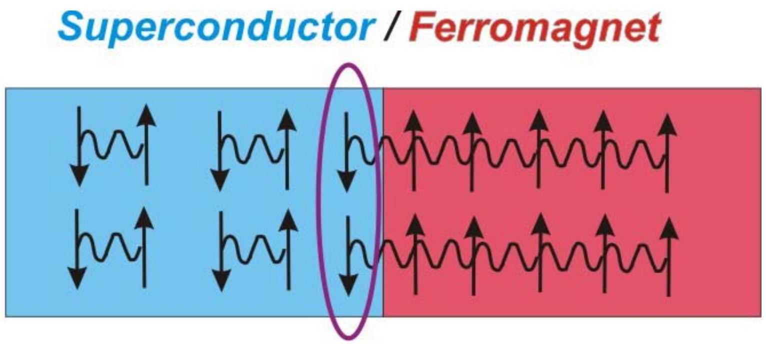

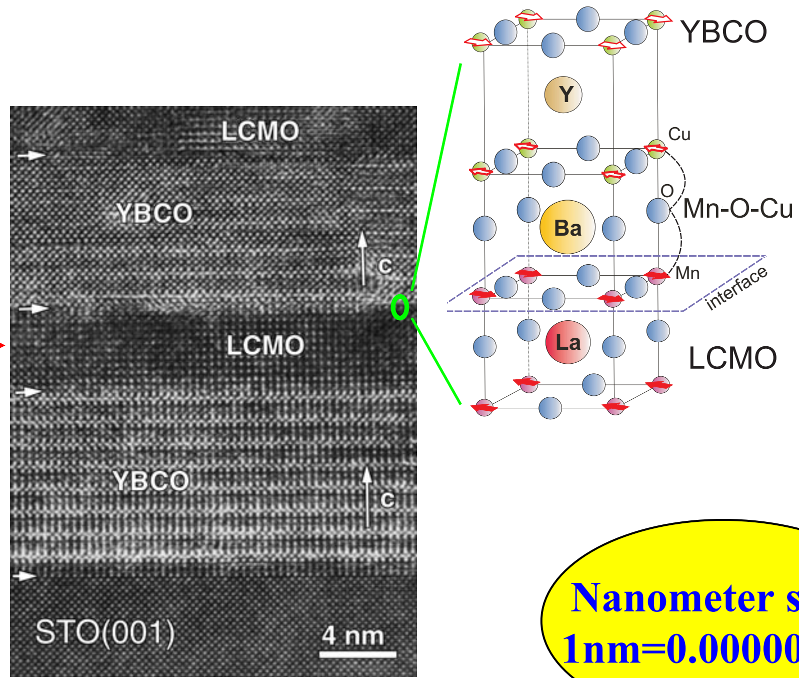

Ferromagnet,
$La_{2/3}Ca_{1/3}MnO_3$

High T_c superconductors
$YBa_2Cu_3O_7$

Nanometer scale:
1nm=0.000001mm

Pulsed Laser Deposition (PLD)
RHEED controlled

Brendan Doggett

Vivek Malik

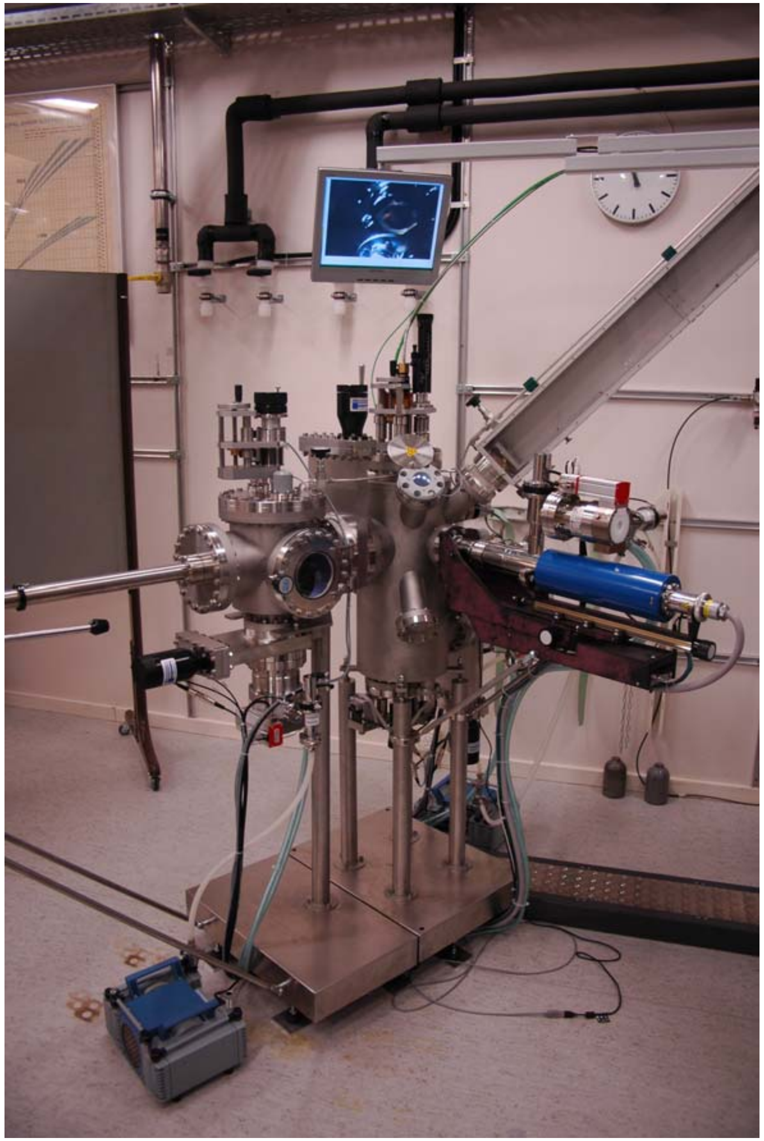

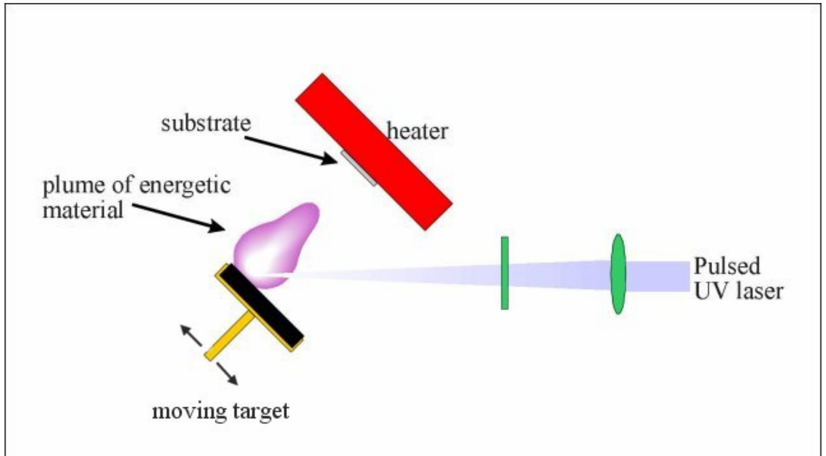

Pulsed Laser Deposition

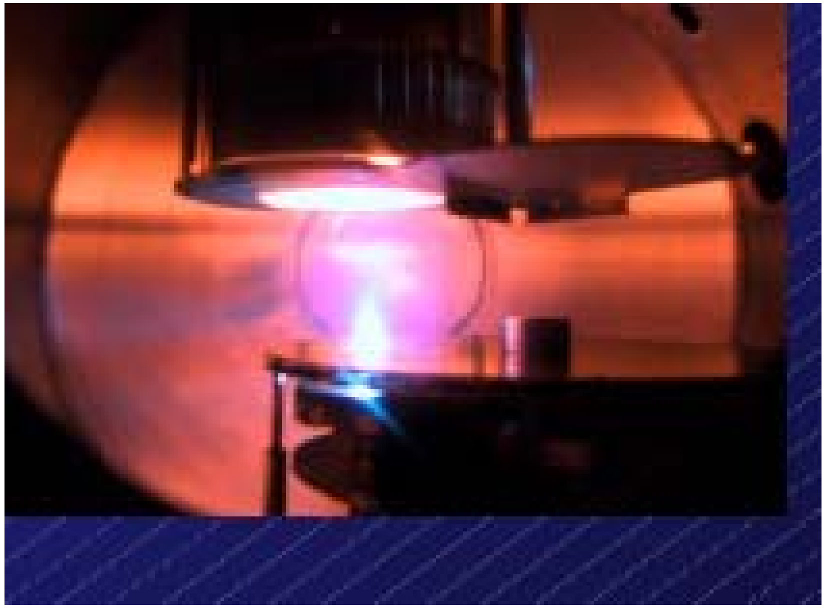

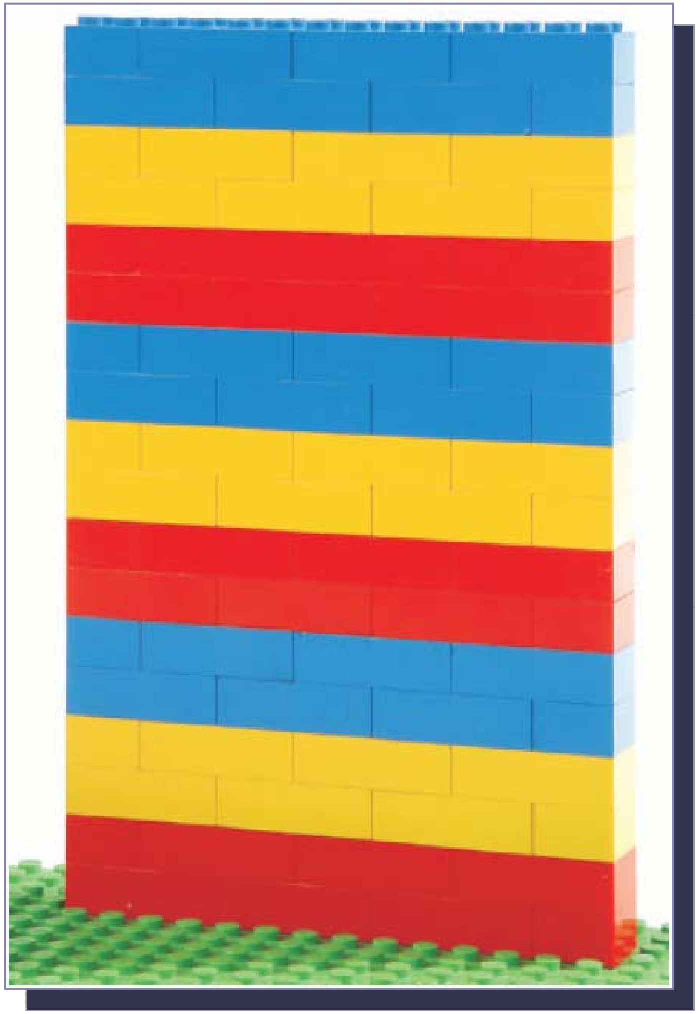

Perovskitartige Oxide:

- Isolatoren
- Metalle
- Supraleiter
- Ferromagneten
- Antiferromagnete
- Ferroelektrika
- Antiferroelektrika
- Multiferroika

……

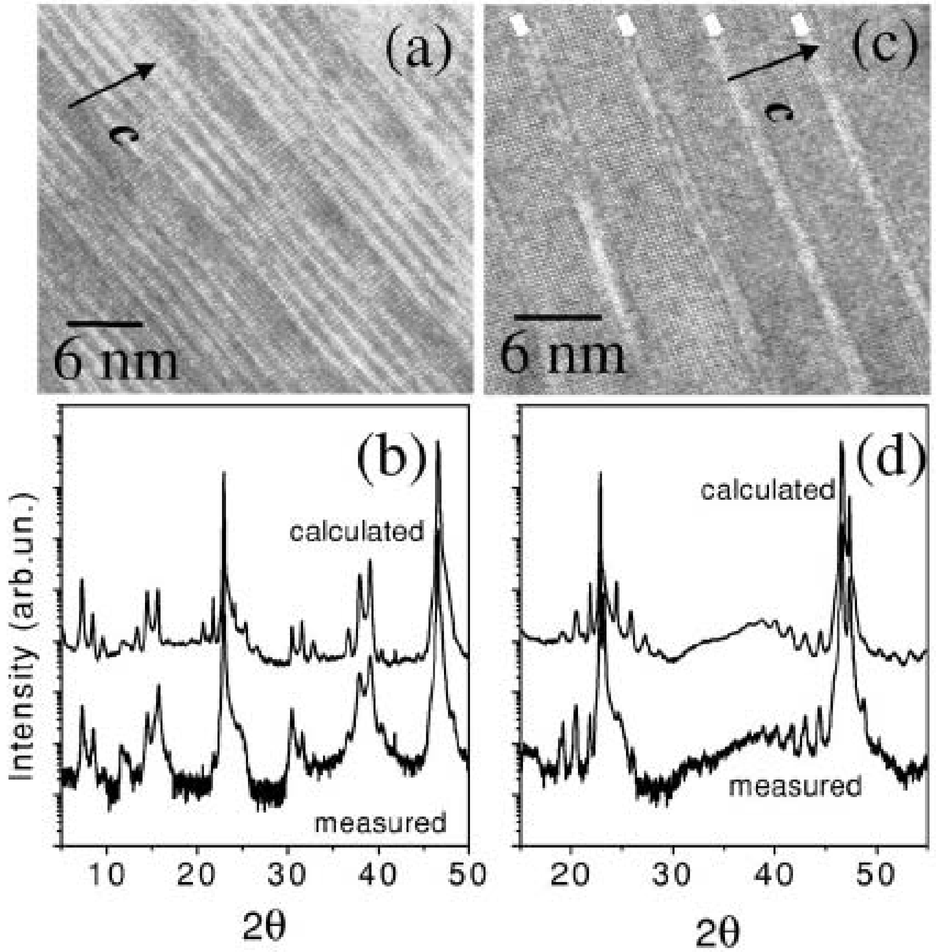

FIG. 1. (a) TEM cross section view of a [LCMO (3 unit cell)/ YBCO (5 unit cell)] superlattice. (b) X-ray diffraction pattern and SUPREX calculated spectra of sample [LCMO (3 unit cell)/YBCO (5 unit cell)]. (c) TEM cross section view of a [LCMO (15 unit cell)/YBCO (1 unit cell)] superlattice. (d) X-ray diffraction pattern and SUPREX calculated spectra of sample [LCMO (15 unit cell)/ YBCO (1 unit cell)].

Z. Sefriui et al., PRB 67, 214511 (2003).

Superconductivity versus Ferromagnetism!

Superconductor **Ferromagnet**

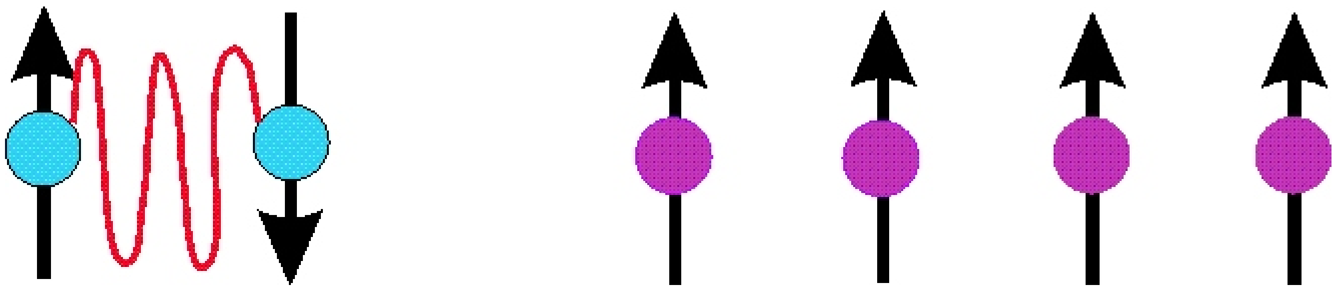

applications:
Faster, more efficient, energy saving, ….

Fundamental science:
fascinating and challenging

New combined SC/FM quantum states.

New devices for example
in quantum computing, etc.

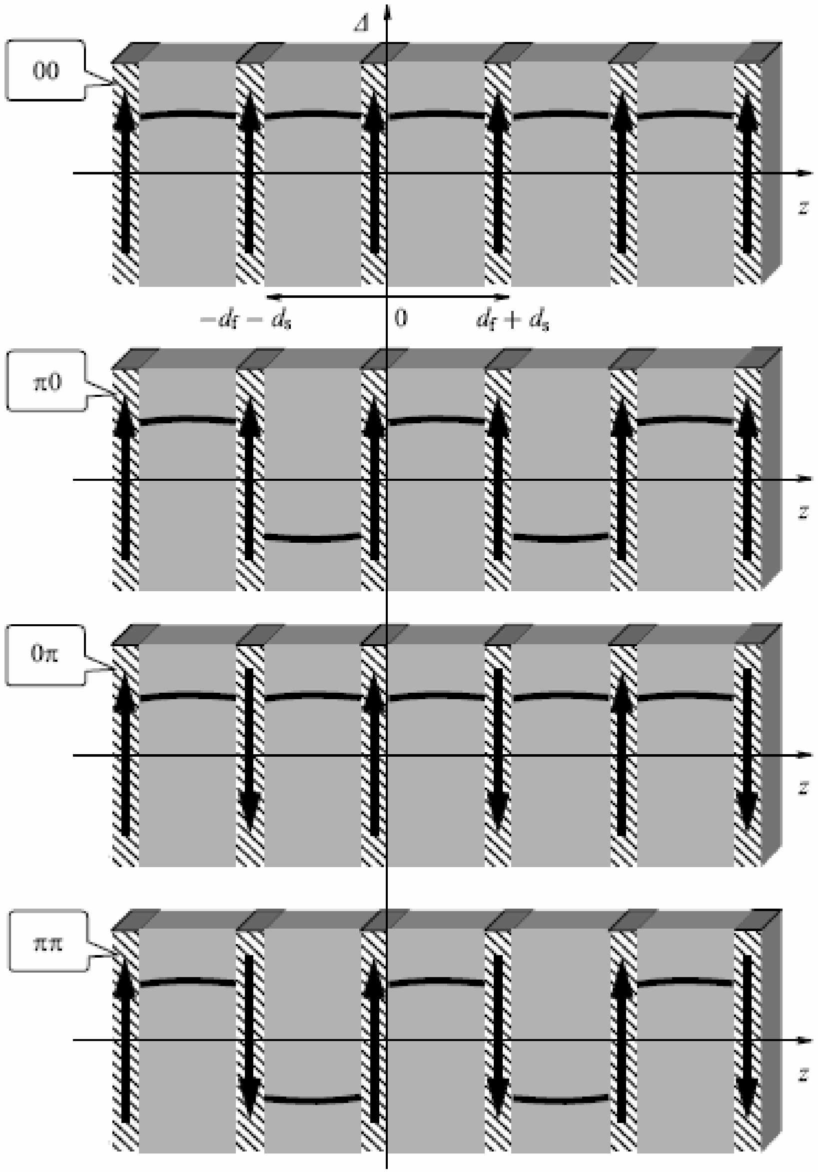

Figure 6. Four possible states of the FM/S superlattice. Horizontal arrows show the unit cell of the superlattice. Solid lines show the behavior of the superconducting order parameter (OP) $\Delta(z)$ in the S layers. In the FM layers, thick solid arrows show the direction of magnetizations, which plays the role of the magnetic OP.

Y.A. Izyumov *et al.*,
Physics Uspekhi **45**, 109 (2002).

Why study SC/FM multilayers from oxides ?

High T_c cuprates:

> High T_c and thus large SC order parameter.

> D-wave order parameter.

> Short SC correlation length.

> Competing magnetic ground state (SDW).

FM manganites

➢High degree of spin polarization.

➢Very good lattice matching.

➢Nearly degenerate FM and non-FM ground states

Phase diagram of cuprate high T_c´s

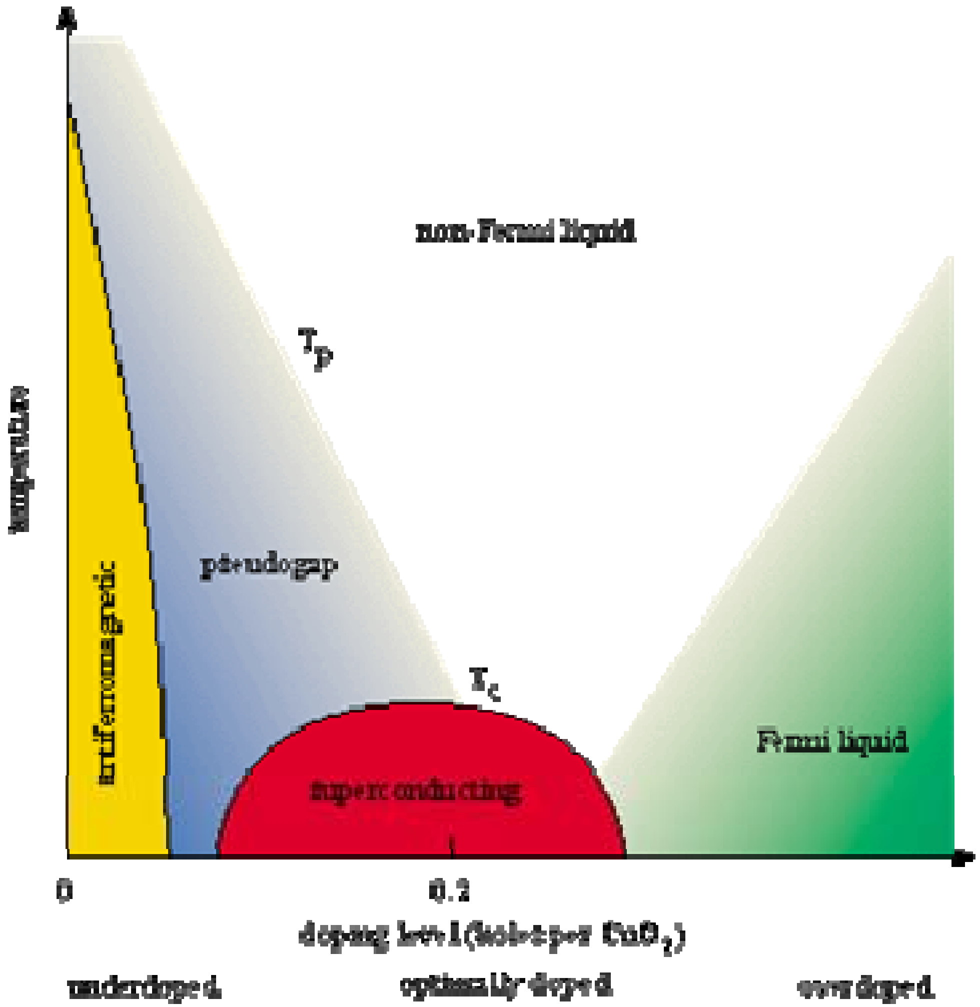

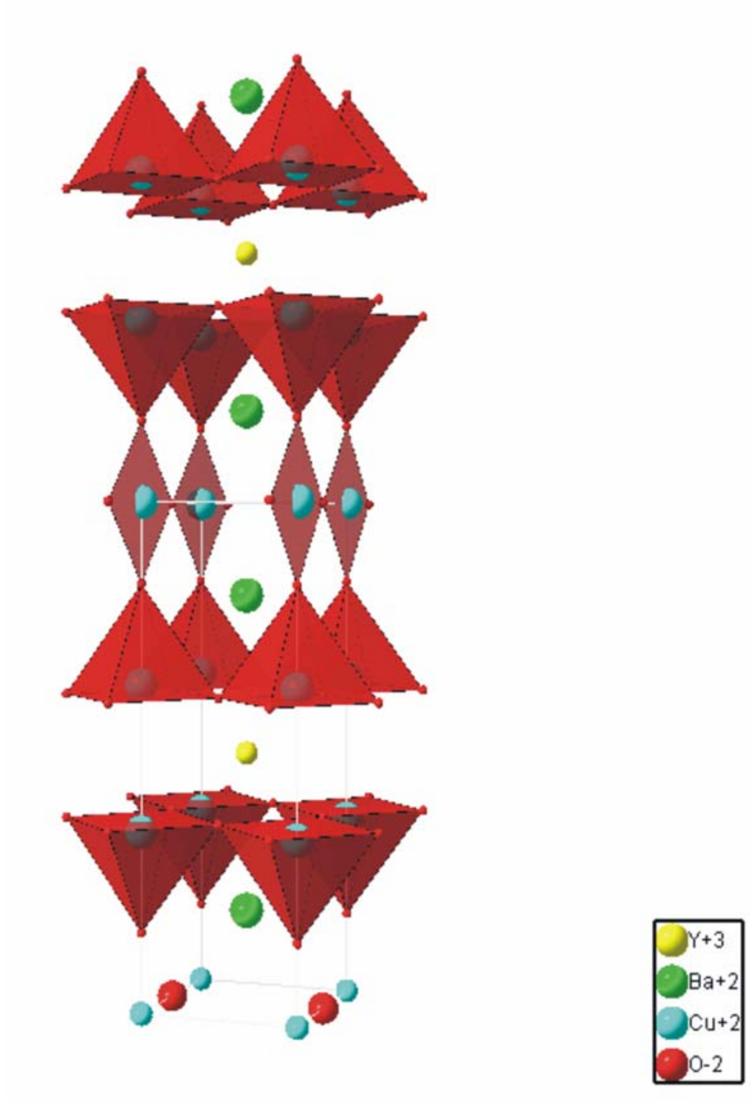

Mott-Hubbard-Insulator

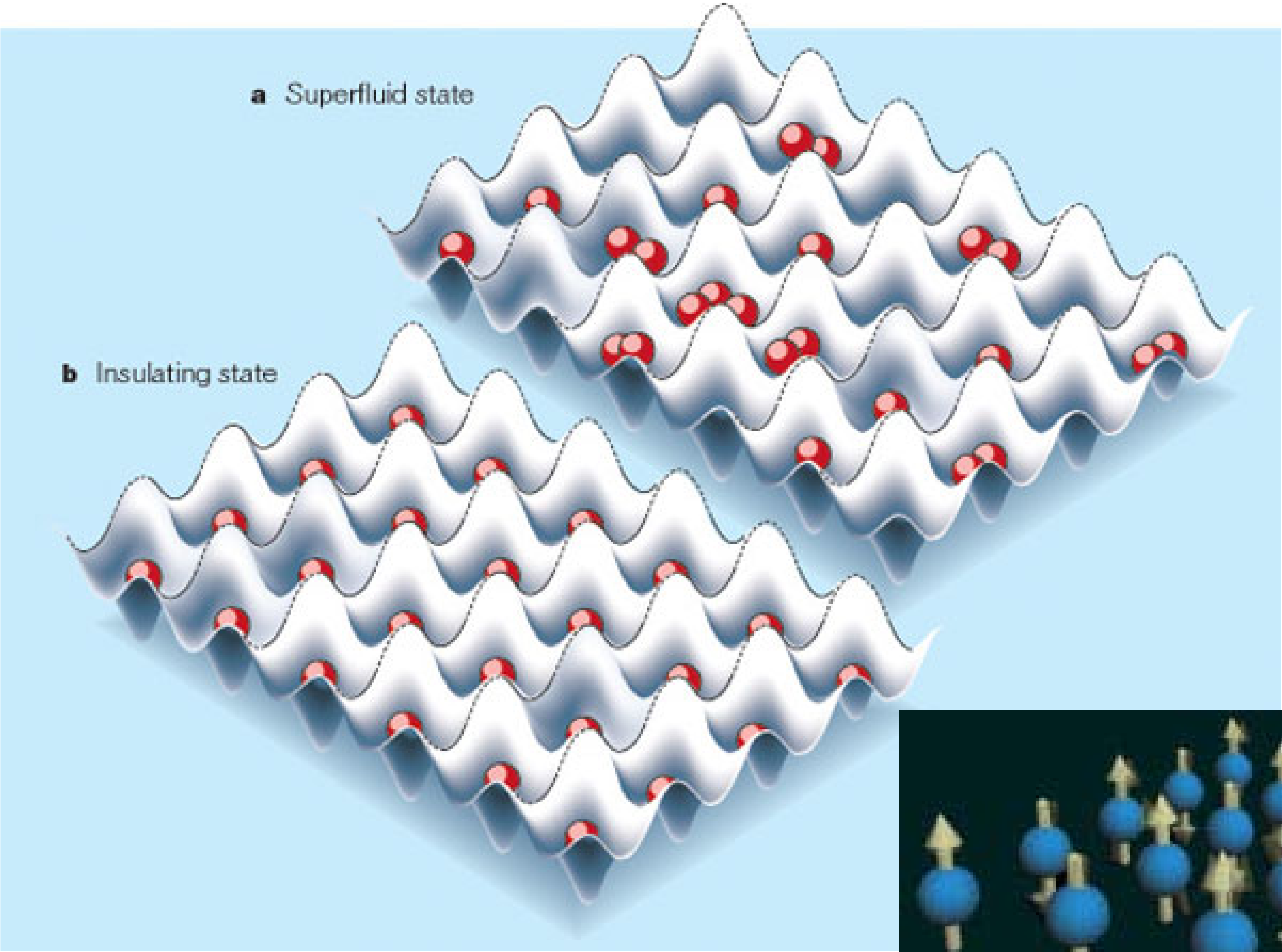

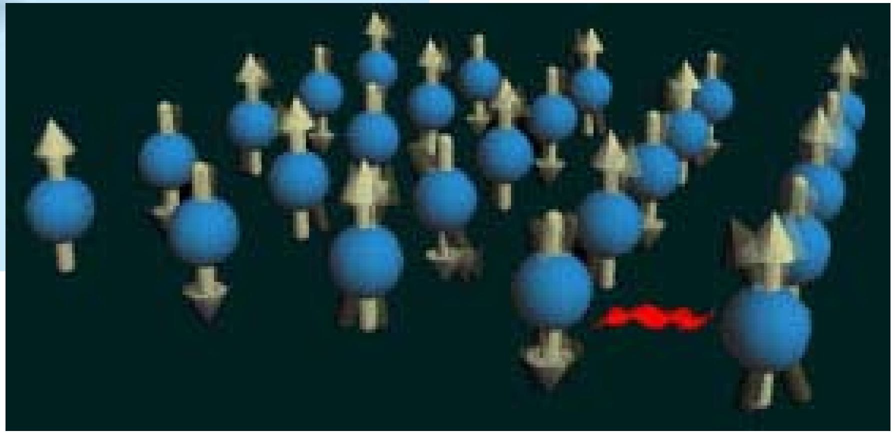

Colosal Magneto-Resistance (CMR) in $La_{2/3}Ca_{1/3}MnO_3$

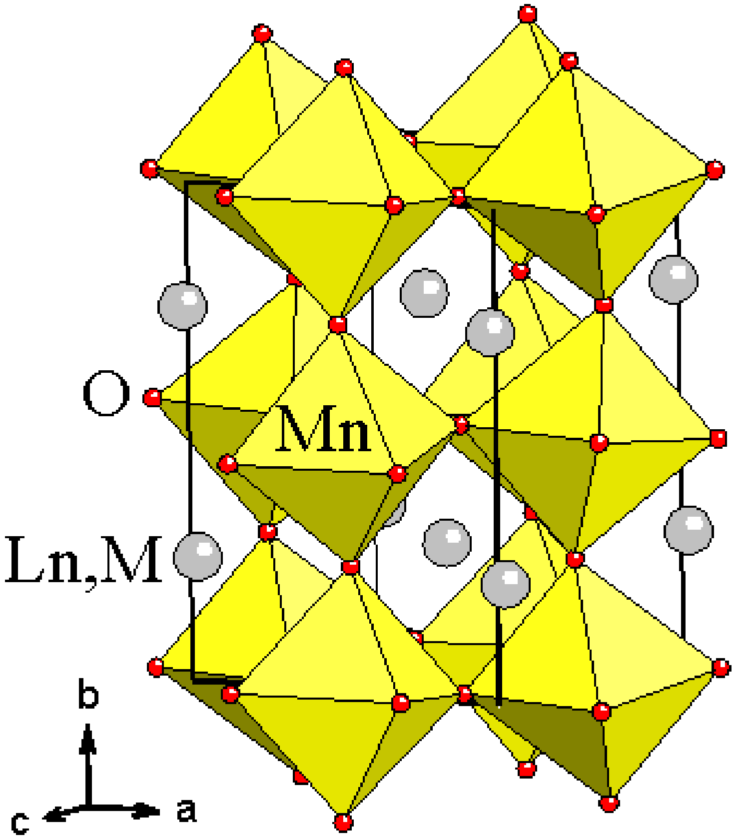

Colossal Magneto-Resistance (CMR)

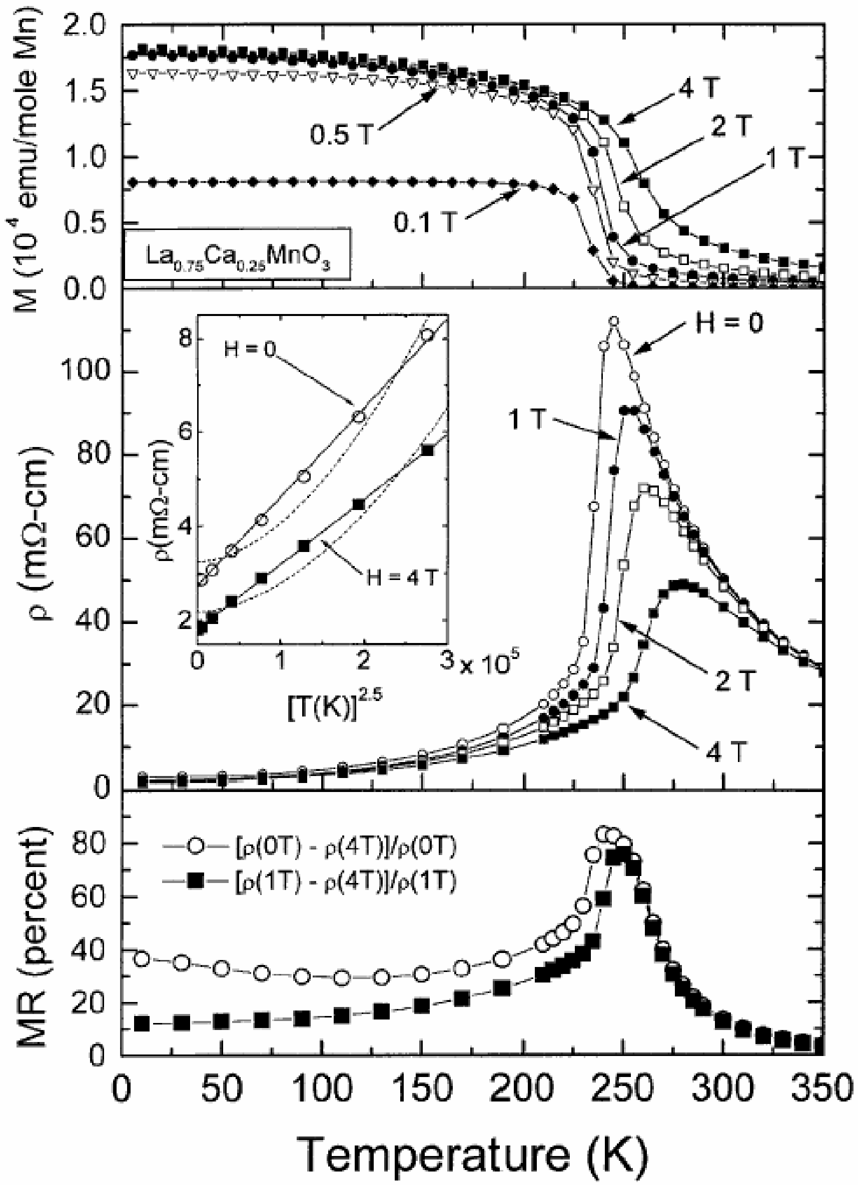

Y. Tokura and Y. Tomioka,
J. Magn. Magn. Mat. **200**, 123 (1999).

Neutron Reflectometry

@ PSI with Jochen Stahn

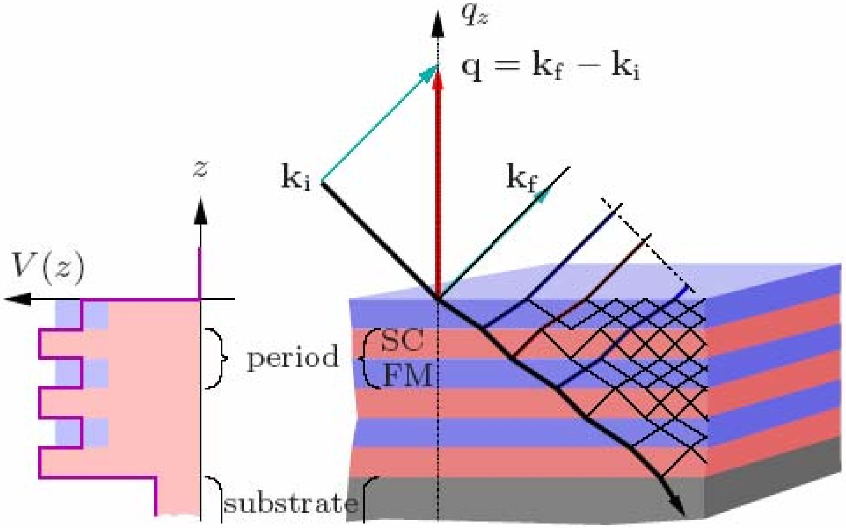

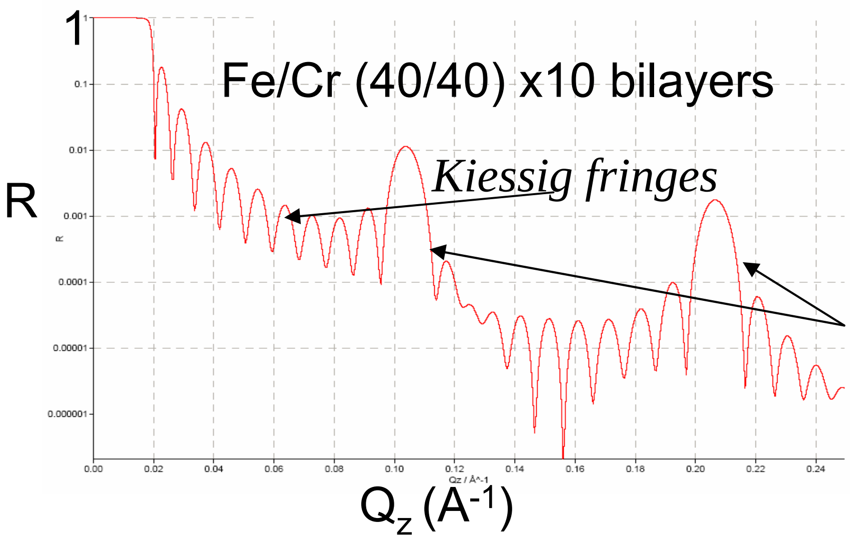

Bragg peaks at $Q_l = \sqrt{Q_c^2 + \left(l \frac{2\pi}{\Lambda}\right)^2}$,

where l is the order of refl. and Λ is a thickness of bilayer

sample Y-LCM68: [YBCO(500 Å)/LCMO(250 Å)]$_5$

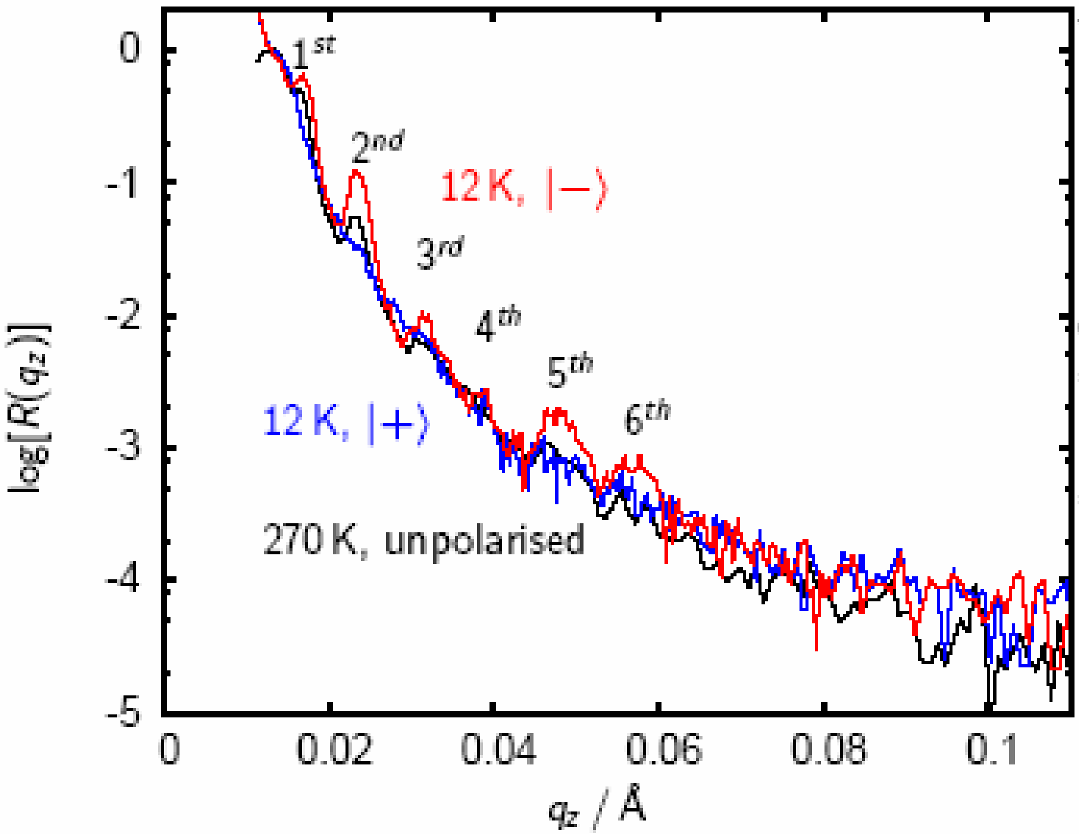

fitted values (RT, unpolarised):

roughness ≈ 5 Å
t_{YBCO} ≈ 520 Å
t_{LCMO} ≈ 180 Å

decreasing resolution with q_z
⇒ decreased d at the edges?

no plateau below q^c
⇒ bent sample?

specular measurements: periodic ml, non-polarised, above T_m

sample: $[\mathrm{YBCO}(100\,\text{Å})/\mathrm{LCMO}(100\,\text{Å})]_7$

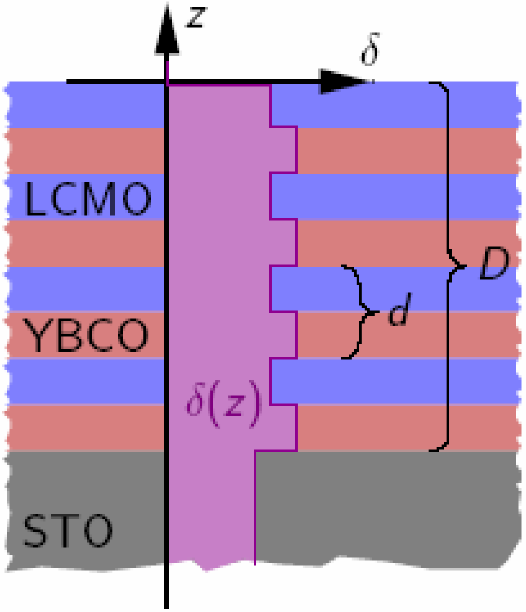

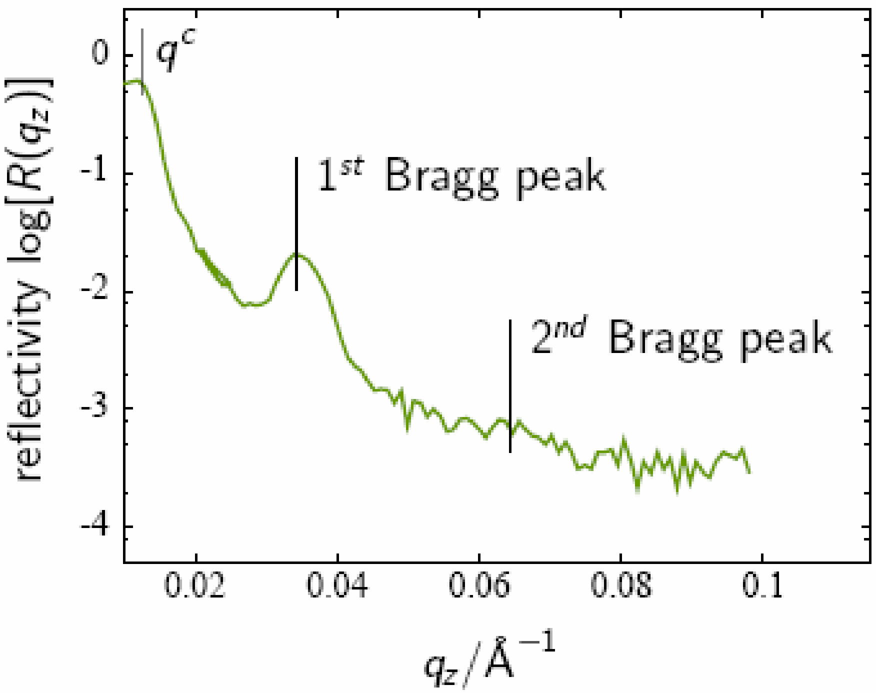

– edge of total external reflection $q_c \propto \sqrt{2\delta}$

– appearance of a Bragg-peak

J. Stahn et al., PRB **71**, R140509 (2005).

specular measurements: periodic ml, non-polarised, various T

sample: $[YBCO(100\,Å)/LCMO(100\,Å)]_7$

T^{Curie}(LCMO)=165 K

T_{sc}=78 K

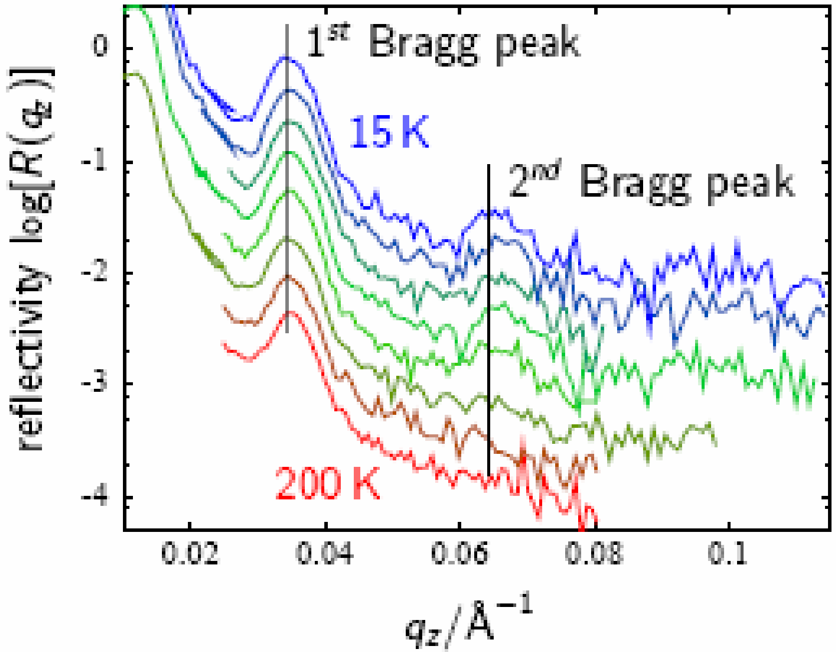

observations:

– shift of q^c below $T_m \approx 165$ K

– increase of 1st Bragg peak for $T_c < T < T_m$

– appearance of a 2nd Bragg peak below T_m

$\Rightarrow$ polarised measurements to probe the magnetic profile

Antiphase exponentially decaying FM moment in YBCO

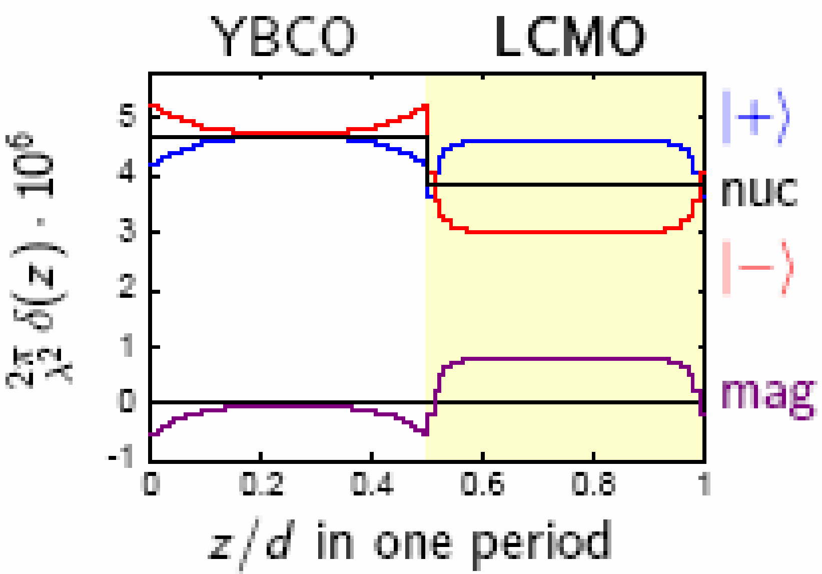

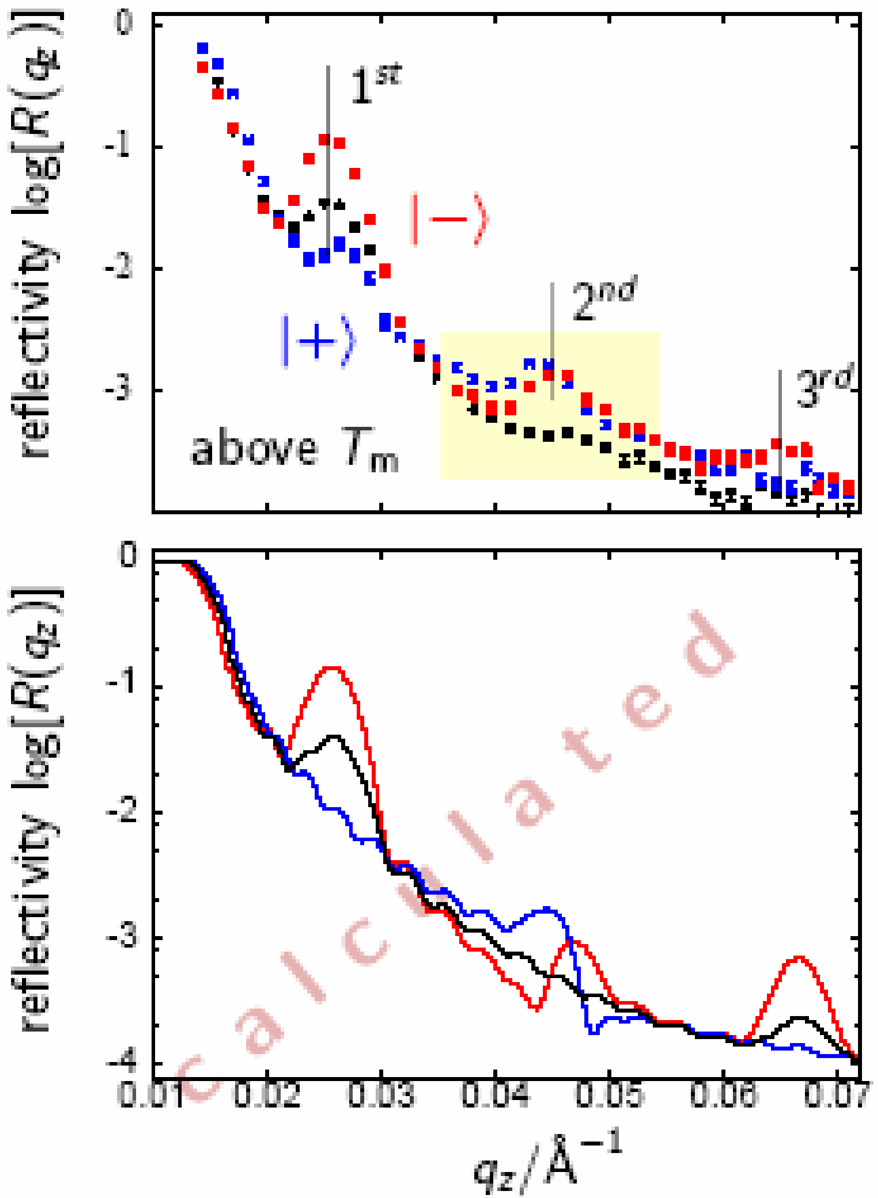

X-ray magnetic circular dichroism (XMCD)

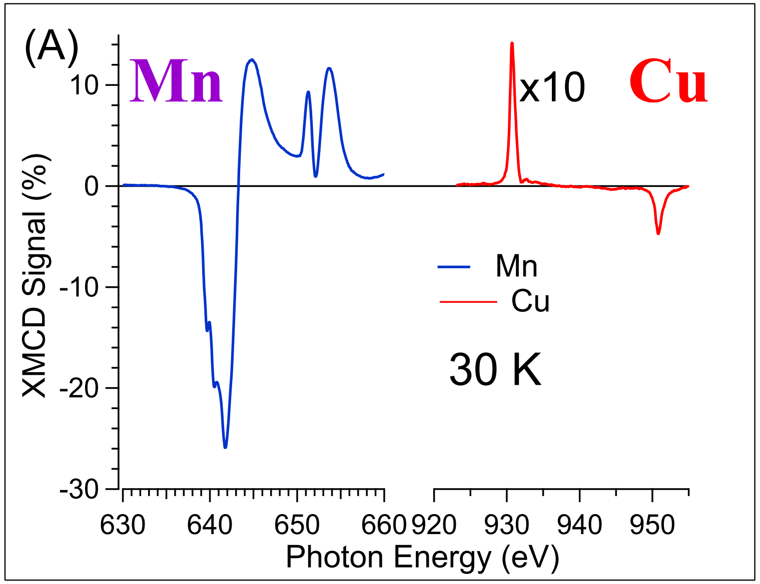

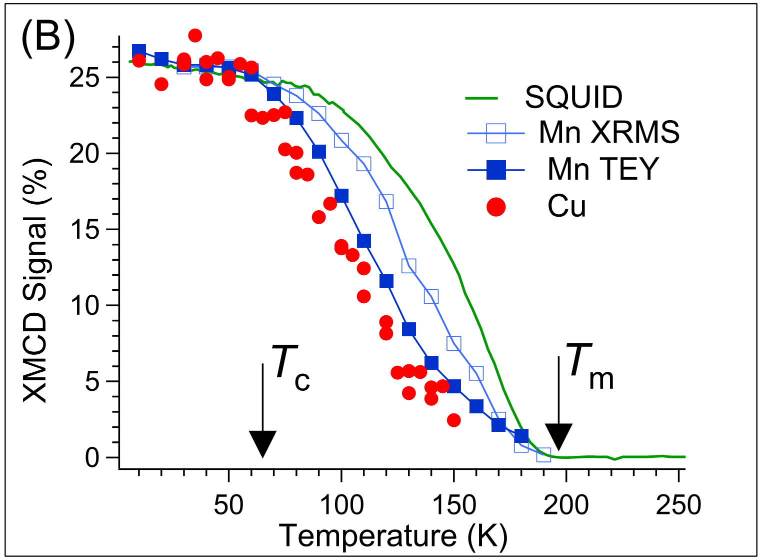

J. Chakhalian et al., Nature Physics **2**, 244 (2006).

Proximity effect between spin singlet and FM

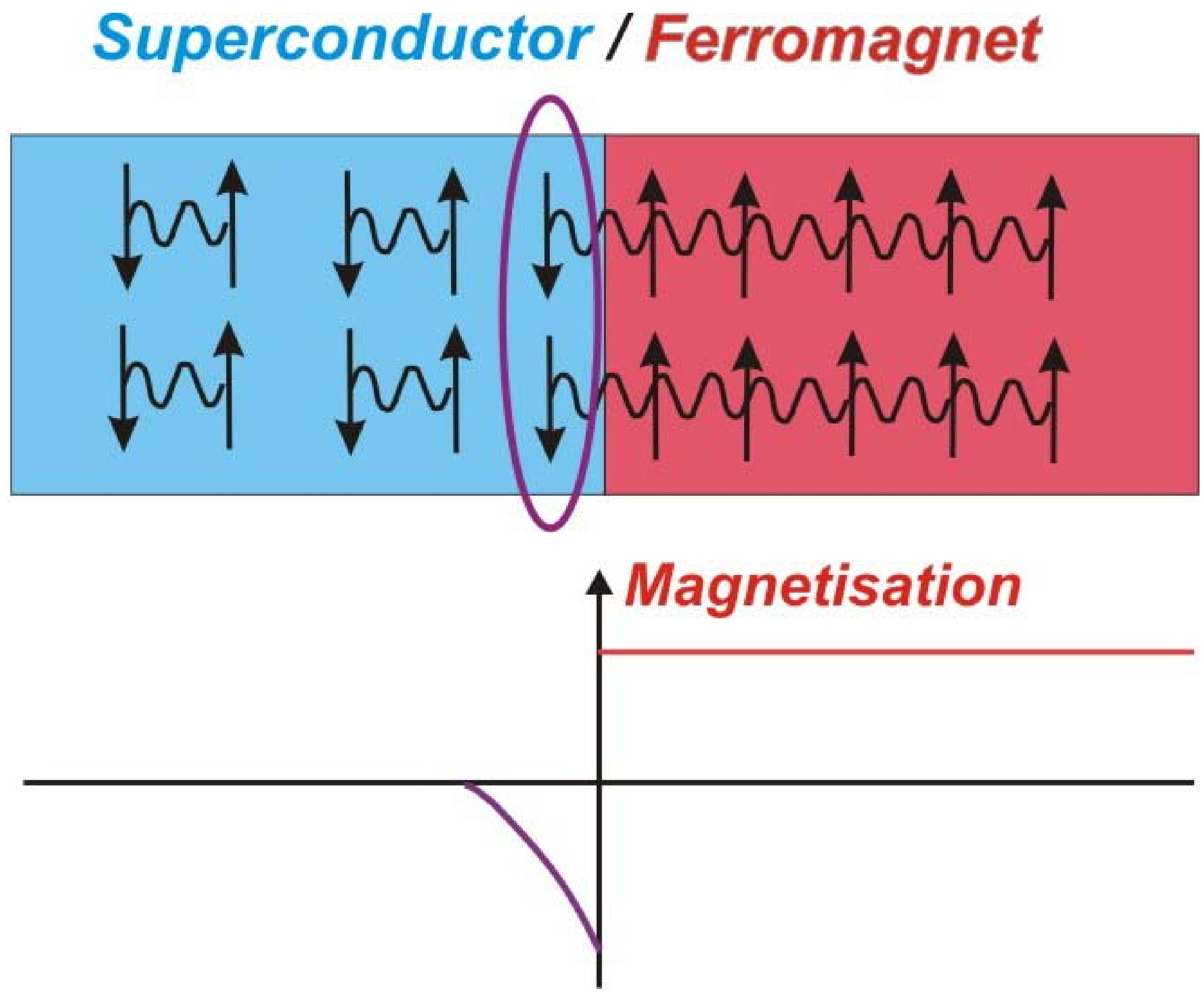

F.S. Bergeret, Phys. Rev. **B 69**, 174504 (2004).

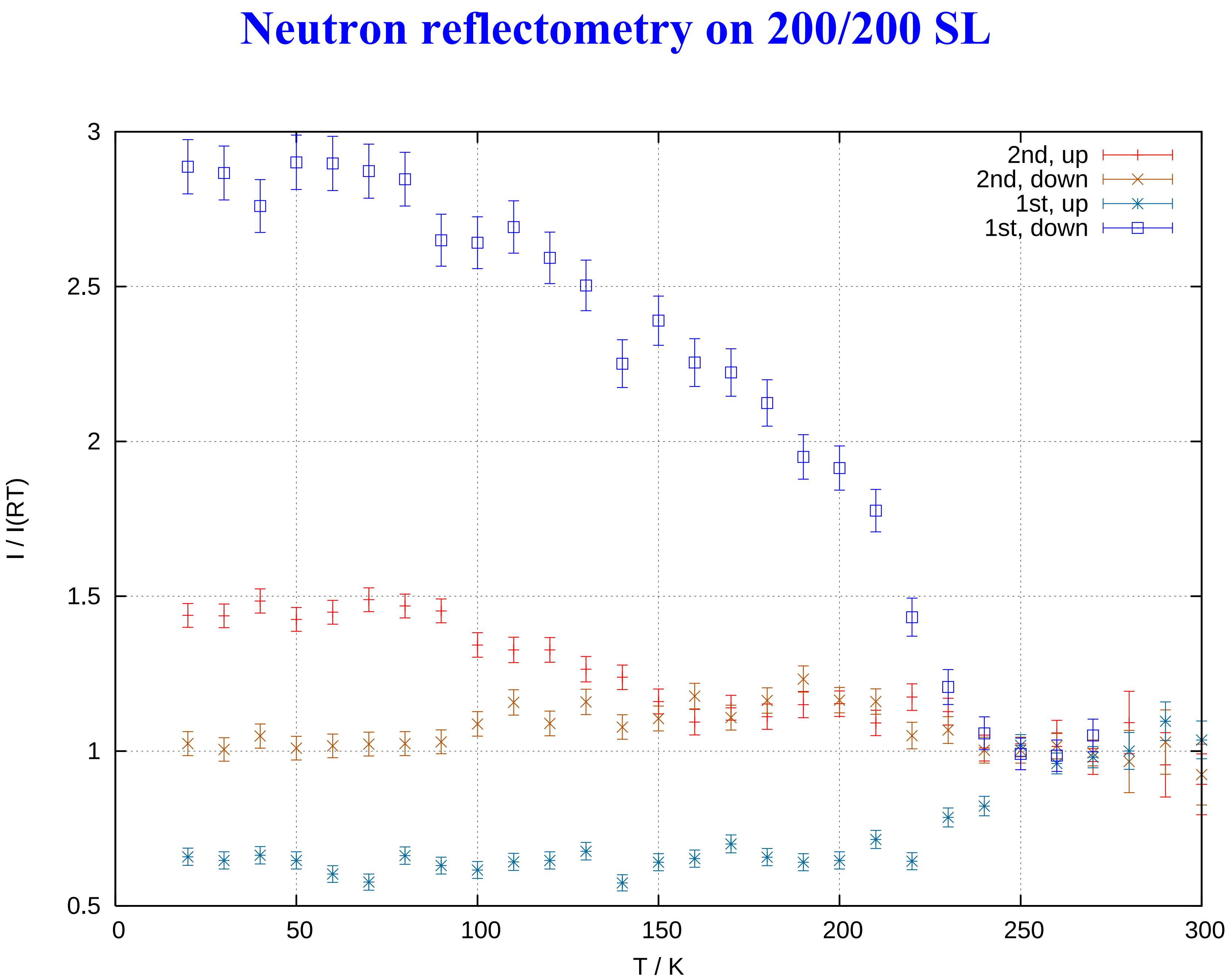

Neutron reflectometry on 200/200 SL
I / I(RT)
T / K
2nd, up
2nd, down
1st, up
1st, down
0
50
100
150
200
250
300
0.5
1
1.5
2
2.5
3

Phase diagram versus carrier concentration

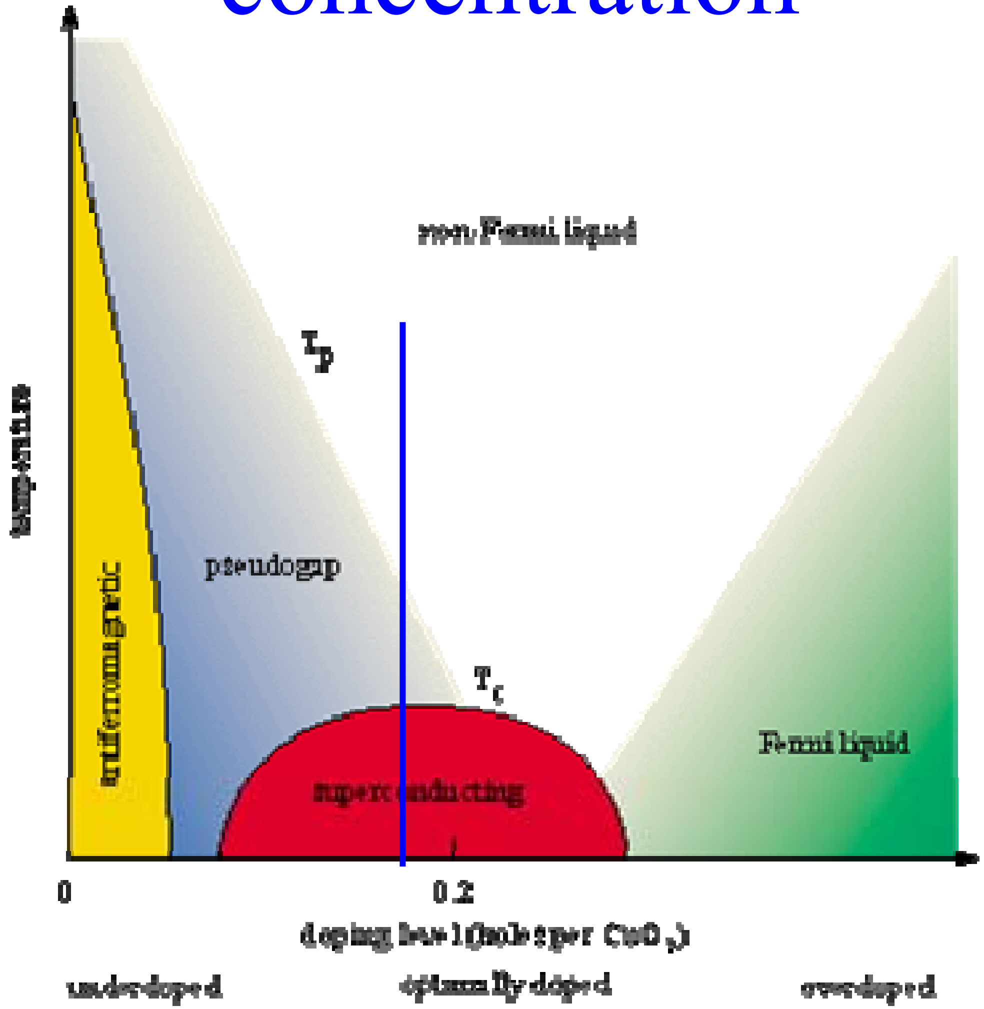

$Y_{0.6}Pr_{0.4}Ba_2Cu_3O_7$ / $La_{2/3}Ca_{1/3}MnO_3$; (100Å /100Å)x9

T_{sc}=40 K, T^{Curie}=190 K

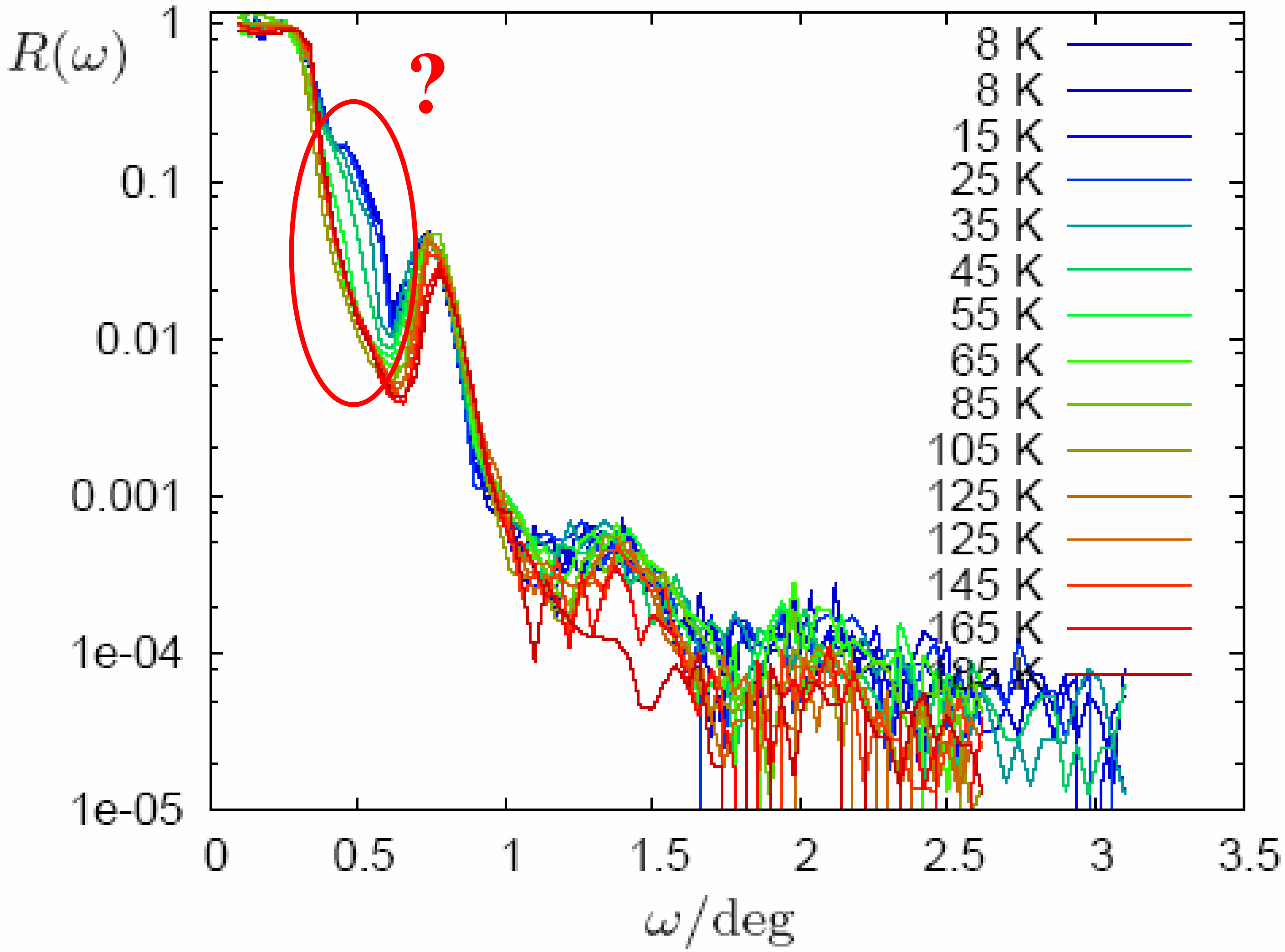

Giant SC-induced modulation of the ferromagnetism

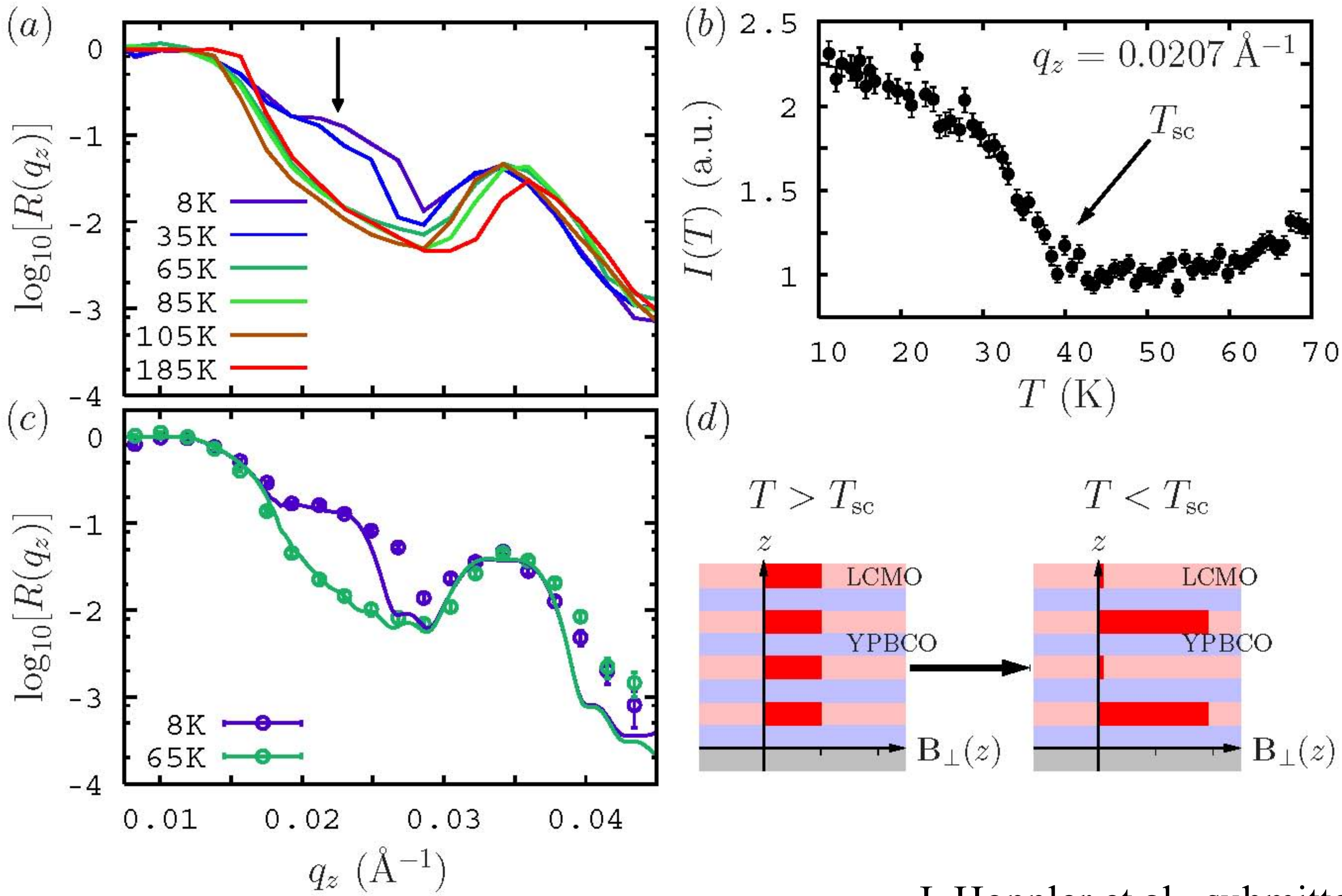

J. Hoppler et al., submitted

But why is the FM so extremely soft?

Unique property of the manganites due to degeneracy of ferromagnetic (metalic) and paramagnetic or antiferromagnetic (insulating) states!

Dramatic variation of magnetisation density with pressure and external magnetic fields are observed!

Double exchange mechanism based on strong on-site Hund coupling → ferromagnetic metal

Jahn-Teller distortion → charge localízation

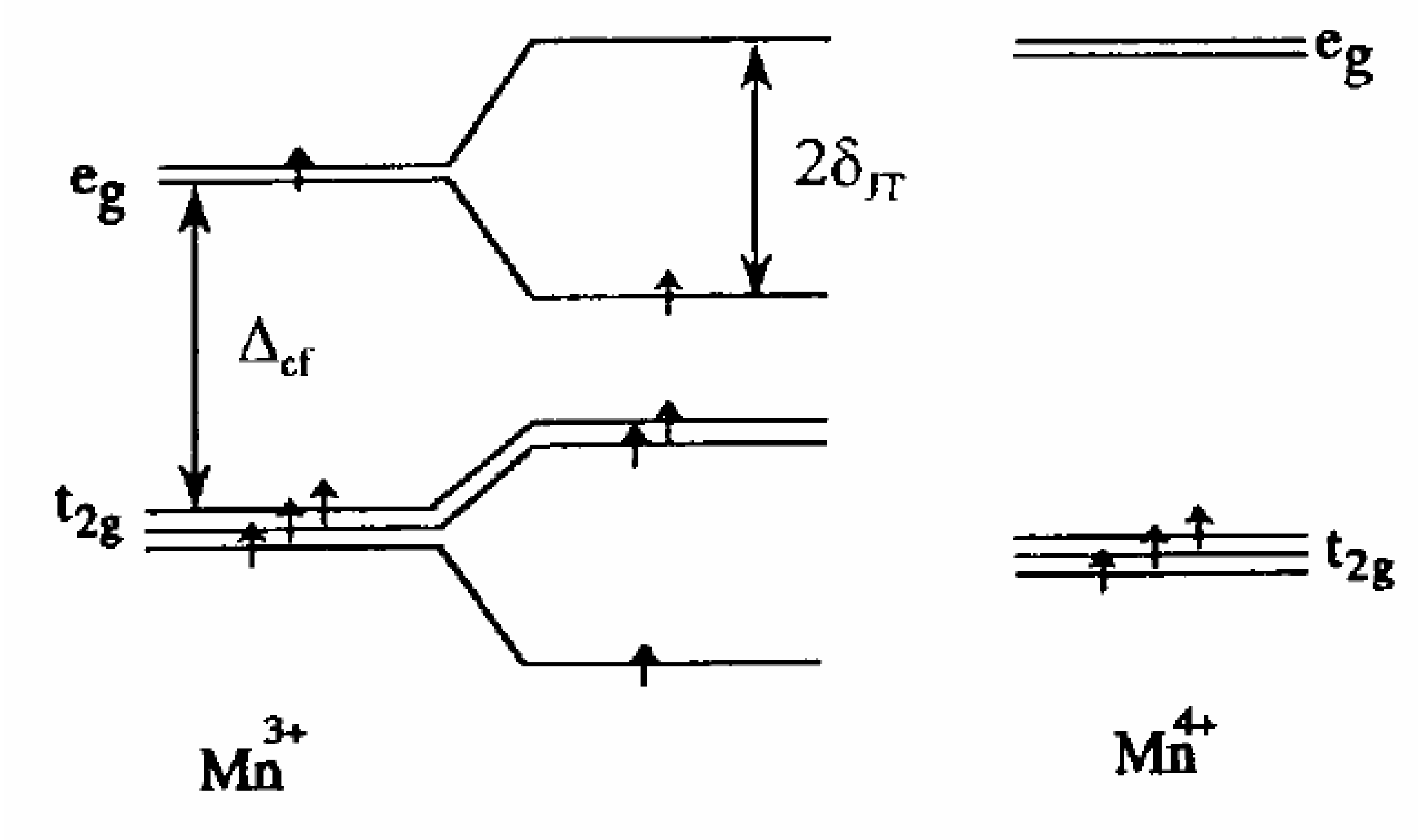

Magnetic field induced insulator-to-metal transition in $Pr_{1-x}Ca_xMnO_3$

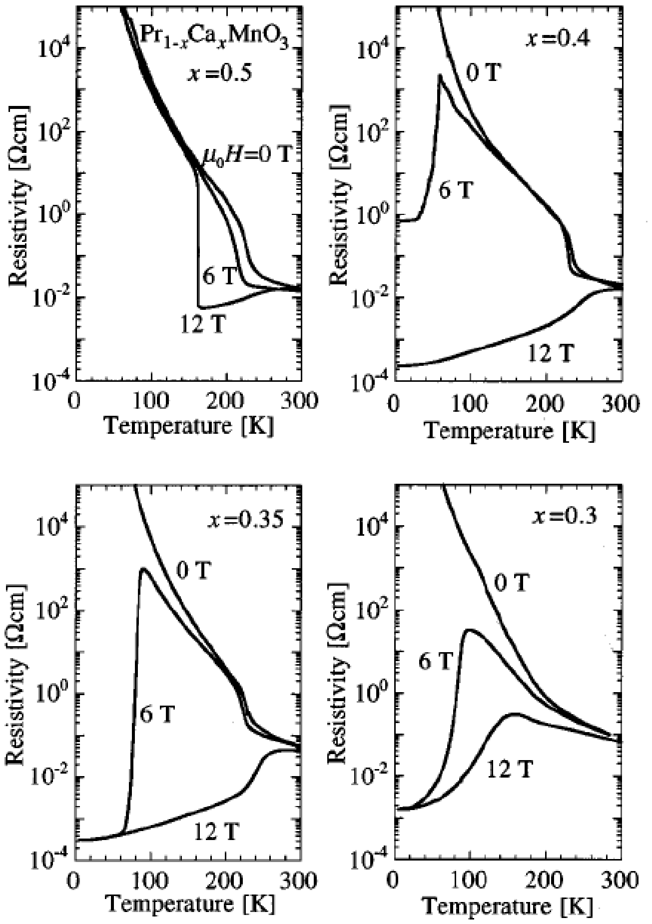

FIG. 2. The temperature dependence of resistivity under $\mu_0 H$=0, 6, and 12 T for $Pr_{1-x}Ca_xMnO_3$ (x=0.5, 0.4, 0.35, and 0.3) crystals. The resistivity was measured in a field cooling (FC) run.

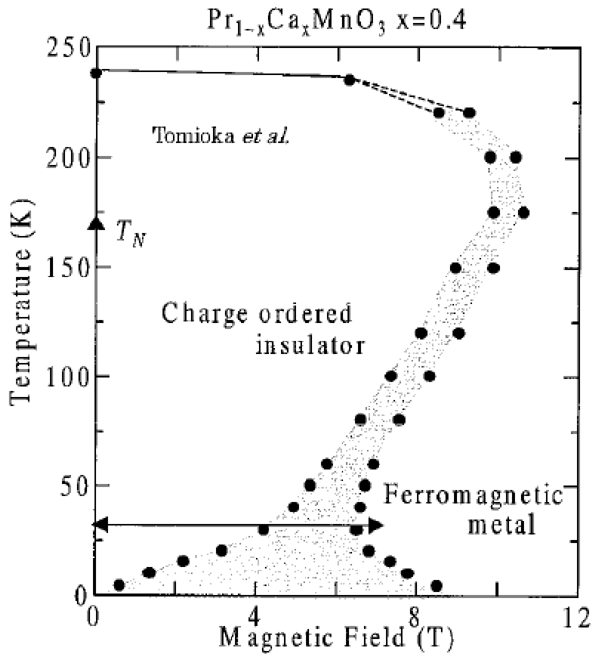

Fig. 11. The magnetic and electronic phase diagram of $Pr_{1-x}Ca_xMnO_3$ (x = 0.4) reproduced from ref [51]. The hatched area shows a field-hesteresis region. A closed triangle denotes the Neel temperature T_N, and an open one the spin-canted antiferromagnetic transition temperature T_{CA}.

Y. Tokura and Y. Tomioka, J. Magn. Magn. Mat. **200**, 123 (1999).

The fractional order Bragg peak is extremely strain sensitive!

$SrTiO_3$ undergoes an antiferrodistrortive transition at 105 K.

Buckling of the substrate that extends through the superlattice → stripy domains (> 100 µm and <20 µm along a- and b-directions, respectively).

X-rays @ SLS

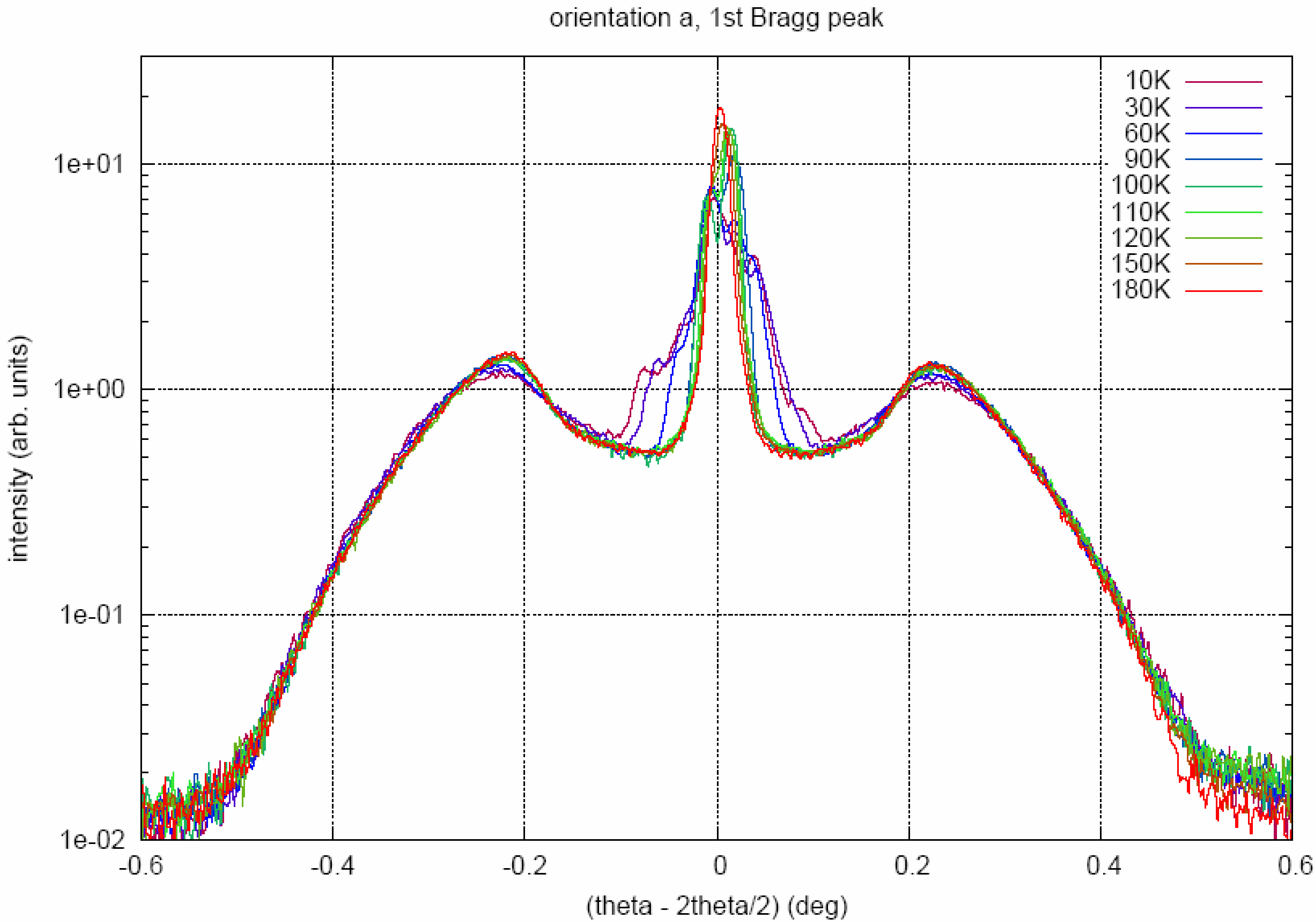

orientation a, 1st Bragg peak
intensity (arb. units)
(theta - 2theta/2) (deg)
1e+01
1e+00
1e-01
1e-02
-0.6
-0.4
-0.2
0
0.2
0.4
0.6
10K
30K
60K
90K
100K
110K
120K
150K
180K

2D Mapping with time-of-flight instrument @ PSI

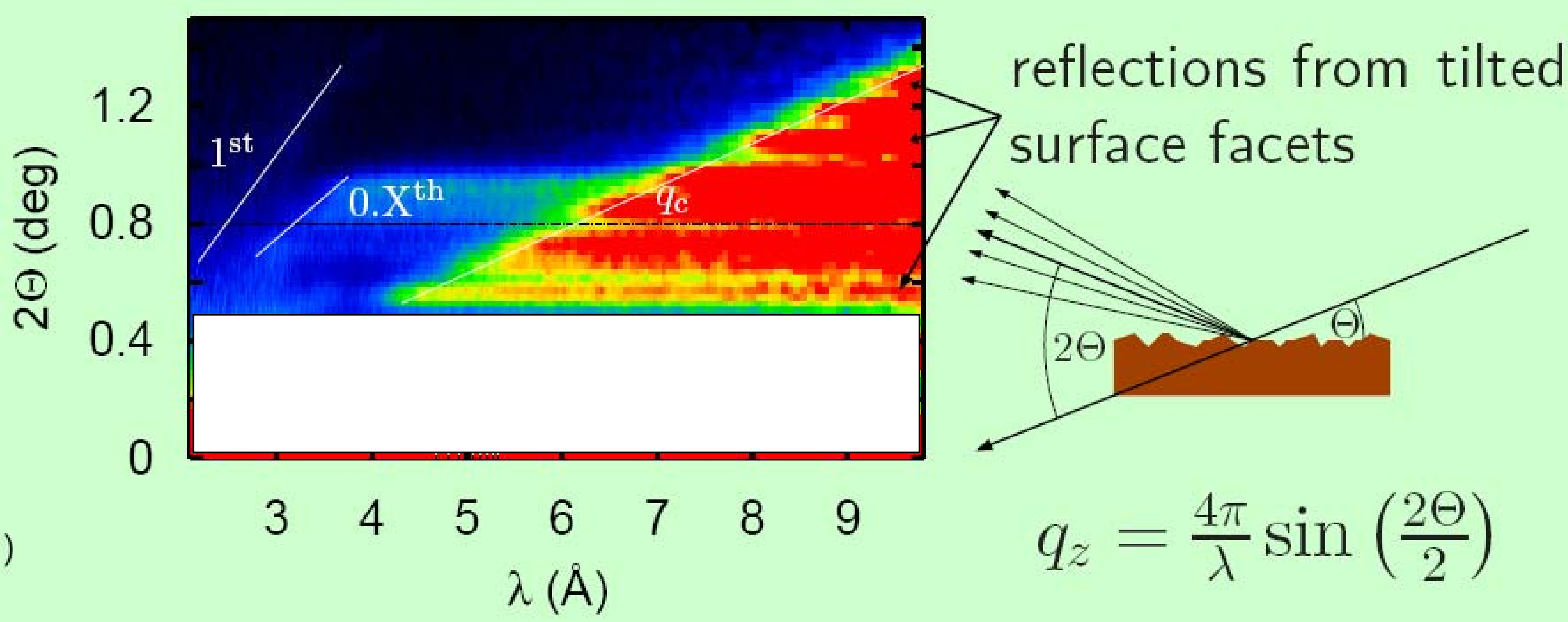

$$q_z = \frac{4\pi}{\lambda} \sin\left(\frac{2\Theta}{2}\right)$$

T=10 K

Strong pressure
4 N/mm²

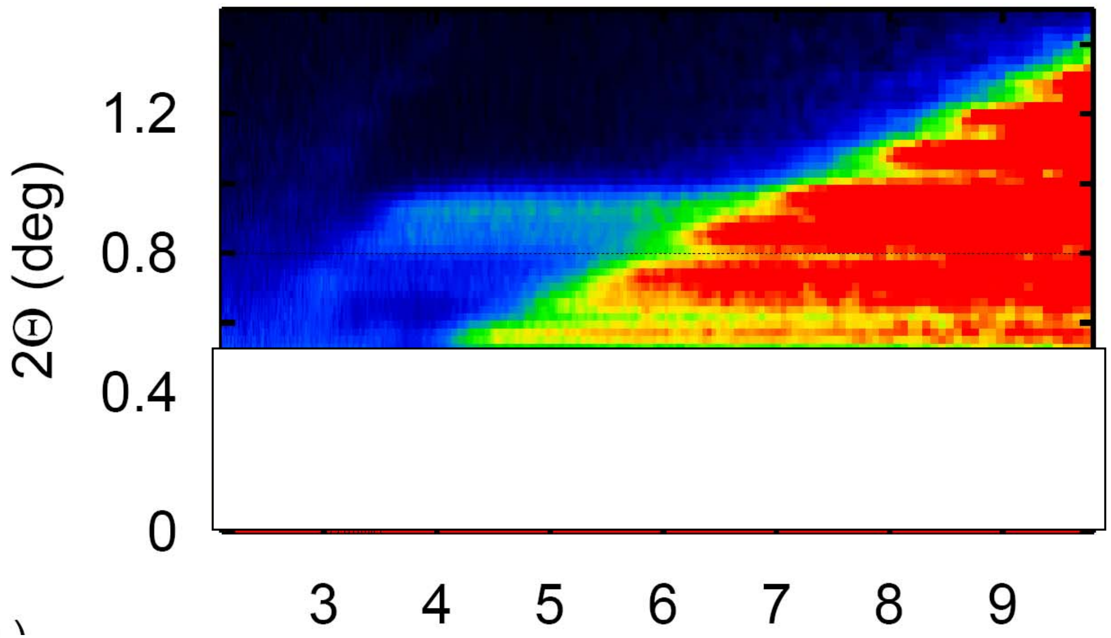

Weak pressure
0.5 N/mm2

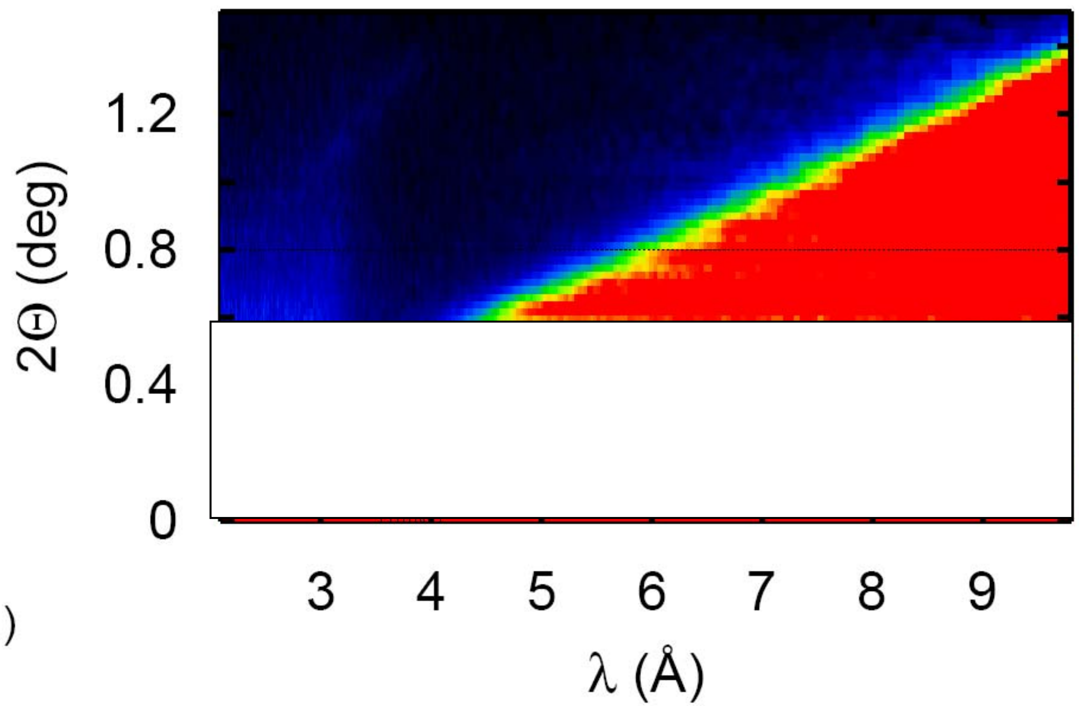

Conclusion

Giant SC-induced modulation of FM order

Very sensitive to strain - may be its good for strain controlled quantum devices?

In any case, it’s a fascinating toy!

Summary

Direct measurement of current-induced spin polarisation in buried non-magnetic layer of a function organic spin valve by muon –spin-rotation

Strong and unusual interaction between high T_c superconductivity and ferromagnetism in oxide mulitlayers.

A Postdoc position is open in my group